

开放量子系统的理论发展与奇特核研究



郭建友
Jian-You Guo

安徽大学 物理与光电工程学院
School of Physical and Optoelectronic
Engineering, Anhui University

Outline

1

Introduction

2

Theoretical framework

- **RMF-CSM**
- **RMF-CGF**
- **RMF-CMR**

3

Application examples

4

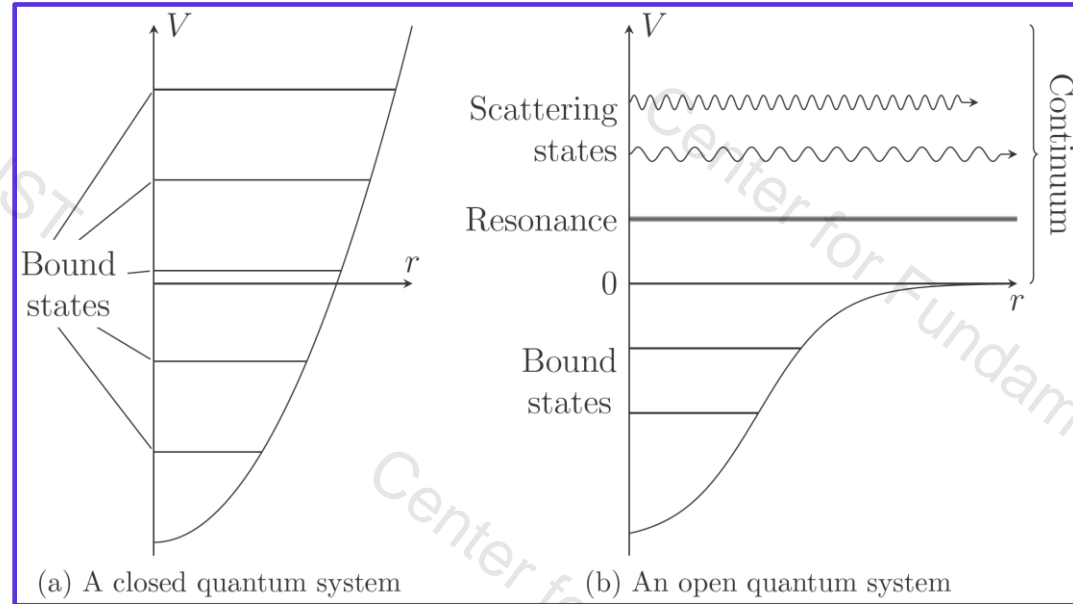
Summary

开放量子系统的含义

When a one-body or multi-body system is constrained, there are two cases, as shown in the diagram on the right.

(a) A closed quantum system

(b) An open quantum system



J. Phys. G: Nucl. Part. Phys. **37** (2010) 064042

Open problems in the theory of nuclear open quantum systems

N Michel¹, W Nazarewicz^{2,3,4}, J Okołowicz⁵ and M Płoszajczak⁶

¹ Department of Physics, PO Box 35 (YFL), FI-40014 University of Jyväskylä, Finland

² Department of Physics and Astronomy, University of Tennessee, Knoxville, TN 37996, USA

³ Physics Division, Oak Ridge National Laboratory, Oak Ridge, TN 37831, USA

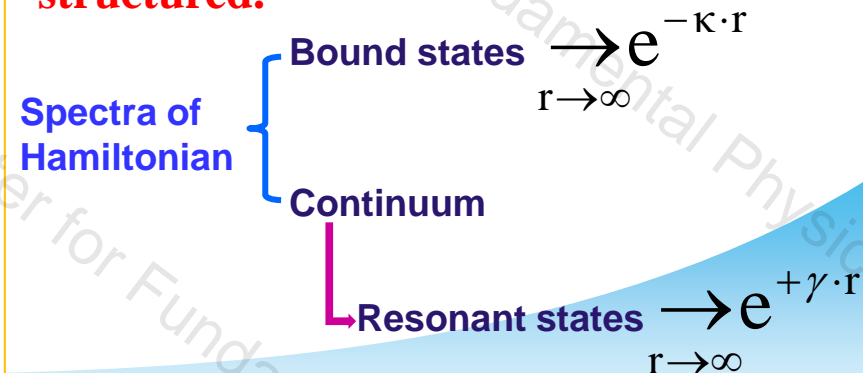
⁴ Institute of Theoretical Physics, University of Warsaw, ul. Hoża 69, PL-00-681 Warsaw, Poland

⁵ Institute of Nuclear Physics, Polish Academy of Sciences, Radzikowskiego 152, PL-31342 Kraków, Poland

⁶ Grand Accélérateur National d'Ions Lourds (GANIL), CEA/DSM—CNRS/IN2P3, BP 55027, F-14076 Caen Cedex, France

E-mail: witek@utk.edu and ploszajczak@ganil.fr

The Hamiltonian of this system is structured.



开放量子系统的研究方法

为了研究开放量子系统，物理学家们发展了一系列理论方法

- ✦ **R-Matrix method**, E.Wigner et al., PR 72, 29 (1947).
- ✦ **K-Matrix method**, J.Humblet et al., PRC 44, 2530 (1991).
- ✦ **The phase-shift method**, J.R.Taylor, *Scattering Theory: The Quantum Theory on Nonrelativistic Collisions* (Wiley, New York, 1972).
- ✦ **Theory of continous spectrum**, NPA 635, 31 (1998); NPA 422, 103 (1984).
- ✦ **J-Matrix method**, H.A.Yamani et al., J.Math.Phys.16, 410 (1975); A.M.Shirokov, et al., PRC79, 014610 (2009).
- ✦ **Coupled-Channel Approach (CCA)**, I.Hamamoto, PRC 72, 024301 (2005); Z.P.Li et al., PRC 81, 034311 (2010).

◆ **Jost function method**

B.N.Lu, E.G.Zhao, and S.G.Zhou, PRL 109, 072501 (2012);

B.N.Lu, E.G.Zhao, and S.G.Zhou, PRC 88, 024323 (2013).

◆ **Real stabilization method (RSM)**

A.U.Hazi and H.S.Taylor, PRA 1, 1109 (1970);

Y.K.Ho, Phys. Rept. 99, 1 (1983).

⇒ **RMF-RSM**

L. Zhang, S.G. Zhou et al., PRC 77, 014312(2008).

◆ **Analytic continuation in the coupling constant (ACCC)**

V.I.Kukulin et al., Theory of Resonances: Principles and Applications (Kluwer Academic, Dordrecht, 1989).

⇒ **RMF-ACCC**

S.C.Yang, J.Meng, S.G.Zhou, CPL 18, 196 (2001).

S.S.Zhang, J.Meng, S.G.Zhou et al., PRC 70, 034308 (2004).

J.Y.Guo, R.D.Wang, and X.Z.Fang, PRC 72, 054319(2005).

J.Y.Guo and X.Z.Fang, PRC 74, 024320 (2006).

★ **Green's function method**

E.N.Economou, Green's Function in Quantum Physics, Springer-Verlag, Berlin, 2006.

Y. Zhang, M. Matsuo, and J. Meng, Persistent contribution of unbound quasiparticles to the pair correlation in the continuum Skyrme-Hartree-Fock-Bogoliubov approach, Phys Rev C, 2011, 83:054301.

⇒ **RMF-GF**

T.T.Sun, S.Q.Zhang, Y.Zhang, J.N.Hu, J.Meng, Green's function method for single-particle resonant states in relativistic mean field theory, Phys.Rev.C 90, 054321(2014). T.T.Sun et al., Phys.Rev.C 95, 054318 (2017).

★ **Complex Scaling Method (CSM)**

Kiyoshi Kato, J. Phys.: Conf. Ser. 49, 73 (2006).

A. T. Kruppa, et al., PRC37, 383 (1988).

B. Gyarmati and A. T. Kruppa, PRC34, 95(1986).

A. T. Kruppa, et al , PRL79, 2217 (1997).

K. Arai, PRC74, 064311 (2006).

Few-body model+CSM

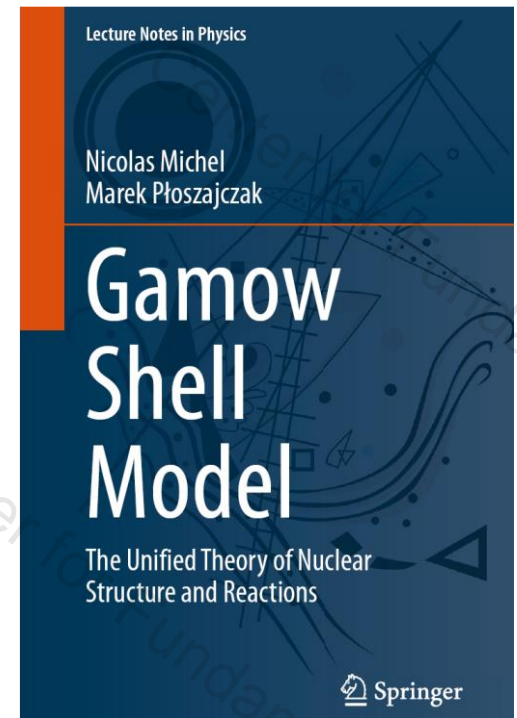
- ✦ Takayuki Myo, et al., Analysis of 6He Coulomb breakup in the complex scaling method, PRC63, 054313(2001)
- ✦ Kenichi Yoshida, Role of low-l component in deformed wave functions near the continuum threshold, PRC72, 064311 (2005)
- ✦ A. T. Kruppa, Scattering amplitude without an explicit enforcement of boundary conditions, PRC75, 044602 (2007)
- ✦ Takayuki Myo, et al., Five-body resonances of 8He using the complex scaling method, PLB691, 150 (2010) Javier von Stecher, Five- and Six-Body Resonances Tied to an Efimov Trimer, Phys.Rev.Lett. 107, 200402 (2011)
- ✦ Takayuki Myo, Five-body resonances in 8He and 8C using the complex scaling method, PRC 104, 044306 (2021)
- ✦ Myagmarjav Odsuren, Doublet $1/2^+$ resonances of 9B in the complex scaling method, PRC 107, 044003 (2023)
- ✦ Takayuki Myo and Kiyoshi Kato, Complex scaling: Physics of unbound light nuclei and perspective, Prog. Theor. Exp. Phys. 2020, 12A101

➤ 很好地描述了轻核晕等奇特现象，如 ^6He , ^6Be , ^7He , ^7B , ^8He , ^8C , ^{10}Li , ^{11}Li

● 少体模型适用于描述轻核（质量数10以下）

Shell model+CSM \Rightarrow Gamow Shell Model

- ✦ N. Michel, et al., **Gamow Shell Model Description of Neutron-Rich Nuclei**, PRL89, 042502 (2002).
- ✦ G. Hagen, et al., **Gamow shell model description of weakly bound nuclei and unbound nuclear states**, PRC 73, 064307 (2006).
- ✦ J. Rotureau, et al., PRL97, 110603 (2006).
- ✦ J.G.Li, N.Michel, B.S.Hu, W.Zuo, and F.R.Xu, **Ab initio no-core Gamow shell-model calculations of multineutron systems**, PRC 100, 054313 (2019)



N. Michel, et al., **Gamow Shell Model**, Springer International Publishing AG 2021.

- **GSM适用于描述轻核到中等质量核**

密度泛函理论 (Density functional theory, DFT)

- *Ab initio*

Navratil, Vary, Barrett Phys. Rev. Lett. 84 (2000) 5728

Bogner, Furnstahl, Schwenk

Prog. Part. Nucl. Phys. 65 (2010) 94

...

- Shell model

Caurier, Martínez-Pinedo, Nowacki, Poves, Zuker,
Rev. Mod. Phys. 77 (2005) 427

Otsuka, Honma, Mizusaki, Shimizu, Utsuno,
Prog. Part. Nucl. Phys. 47(2001)319

Brown, Prog. Part. Nucl. Phys. 47 (2001) 517

...

- Density functional theory

Jones and Gunnarsson,

Rev. Mod. Phys., 61 (1989) 689

Bender, Heenen, Reinhard,

Rev. Mod. Phys., 75 (2003) 121

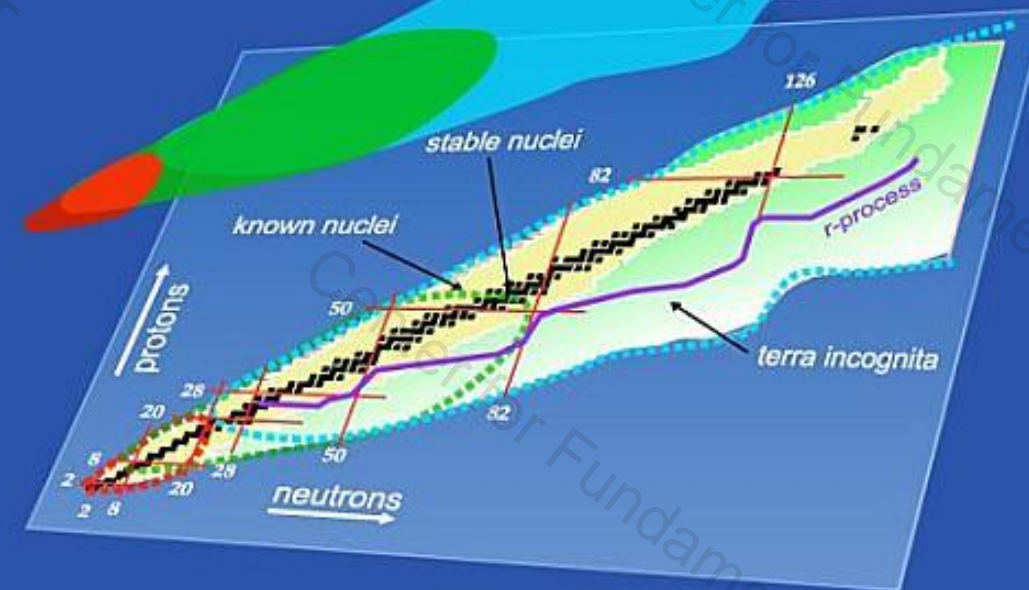
Ring, Prog. Part. Nucl. Phys. 37(1996)193

Meng, Toki, Zhou, Zhang, Long, Geng,

Prog. Part. Nucl. Phys. 57 (2006) 470

...

Nuclear Landscape

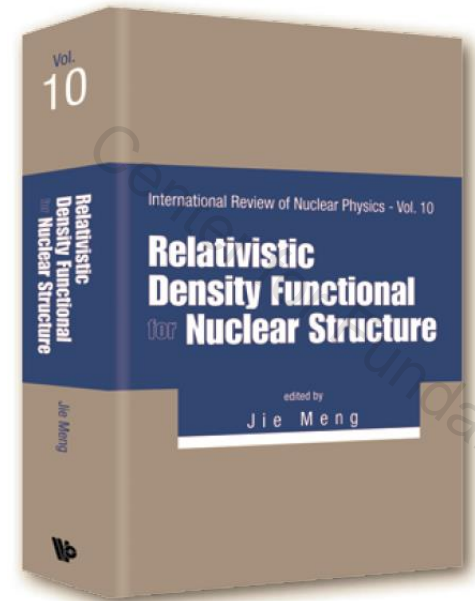
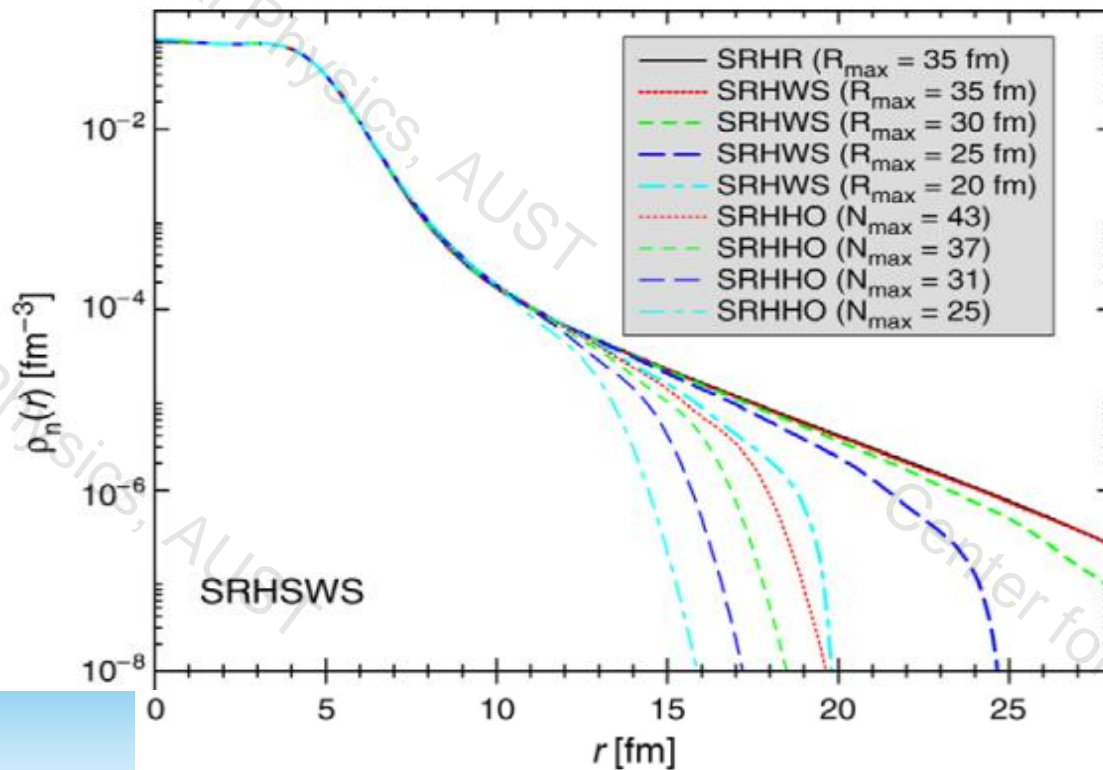


密度泛函理论有望给出核素图上所有原子核性质的统一描述。

Deficiencies of conventional DFT

- 计算的密度分布，其弥散性依赖于盒子的大小。
- 计算的密度分布，其弥散性与基的大小也相关。
- 描述原子核的束缚态很成功，但描述原子核的共振态和散射态遇到困难。

S.G.Zhou et al., PRC 68, 034323 (2003)



Relativistic Density Functional for Nuclear Structure, International Review of Nuclear Physics Vol 10 (World Scientific, 2016)

Improvements to conventional DFT

增加盒子半径或改进基函数

改进基函数

HO

$$\psi_i(\mathbf{r}, s, t) = \begin{pmatrix} f_i(r) \Phi_{l_i j_i m_i}(\theta, \phi, s) \\ i g_i(r) \tilde{\Phi}_{\tilde{l}_i j_i m_i}(\theta, \phi, s) \end{pmatrix} \chi_{t_i}(t)$$

$$\Phi_{l_j m}(\theta, \phi, s) = [\chi_{1/2}(s) \otimes Y_l(\theta, \phi)]_{jm}$$

$$f_i(r) = \sum_{n=0}^{n_{\max}} f_n^{(i)} R_{nl_i}(r, b_0), \quad g_i(r) = \sum_{\tilde{n}=0}^{\tilde{n}_{\max}} g_{\tilde{n}}^{(i)} R_{\tilde{n} \tilde{l}_i}(r, b_0)$$

$$R_{nl}(r, b_0) = b_0^{-3/2} R_{nl}(\xi) = b_0^{-3/2} \mathcal{N}_{nl} \xi^l L_n^{l+1/2}(\xi^2) e^{-\xi^2/2}$$

$$\phi_i \propto e^{-ar^2}$$

$$\xi = r/b_0$$

THO

$$\phi_i \propto e^{-ar}$$

M.V. Stoitsov et al., *Comput. Phys. Comm.* **167** (2005) 43;

M.V. Stoitsov et al., *Comput. Phys. Comm.* **184** (2013) 1592

WS

$$\phi_i(r), \quad r < R$$

S.G. Zhou, J. Meng, P. Ring, E.G. Zhao, *Phys. Rev. C* **82**, 011301 (2010)

Attempts to develop a unified DFT

- ★ **RMF-S**, Sandulescu, Geng, et al., PRC68, 054323 (2003);
- ★ **RMF-ACCC**, Zhang, Meng, et al., PRC70, 034308 (2004);
- ★ **RMF-RSM**, Zhang, Zhou, et al., PRC77, 014312 (2008);
- ★ **RMF-CSM**, Guo, Fang, et al., PRC82, 034318 (2010);
- ★ **RMF-GF**, Sun, Zhang, et al., PRC90, 054321 (2014);
- ★ **RMF-CGF**, Shi, Guo, et al., PRC92, 054313 (2015);
- ★ **RMF-CMR**, Li, Guo, et al., PRL117, 062502 (2016).

- 如何统一描述束缚态、共振态和连续谱以及它们之间的耦合，
- 如何发展稳定核和奇特核的统一理论，

都是待解决的重要问题
(open problems)。

Gamow state

For an open quantum system, there are bound, resonant, and scattering states.

The corresponding wavefunctions can be written as

$$\psi(t, \mathbf{r}) = \psi_t(t)\psi_r(\mathbf{r})$$

The wavefunction evolves according to the time-dependent Schrödinger equation

$$i\hbar \frac{\partial}{\partial t} |\psi\rangle = H |\psi\rangle$$

$$\psi(t, \mathbf{r}) = \exp\left(-\frac{iE}{\hbar}t\right)\psi(0, \mathbf{r})$$

When the energy E is real, the exponential factor is just a phase and the probability of finding the particle at a given \mathbf{r} is unchanged over time

$$|\psi(t, \mathbf{r})|^2 = |\psi(0, \mathbf{r})|^2$$

However, if the energy is complex

$$E = E_0 - i\frac{\Gamma}{2}$$

The probability of finding the particle decays exponentially with time

$$|\psi(t, \mathbf{r})|^2 = \left| \exp\left(-\frac{iE_0}{\hbar}t\right) \exp\left(-\frac{\Gamma}{2\hbar}t\right) \psi(0, \mathbf{r}) \right|^2 = \exp\left(-\frac{\Gamma}{\hbar}t\right) |\psi(0, \mathbf{r})|^2$$

The state is claimed as resonant state (Gamow state) with half-life

$$T_{1/2} = \frac{\hbar \ln 2}{\Gamma}$$

Where the parameter Γ is called the width of the resonance.

The RMF-CSM formalism

Relativistic mean field theory (RMF)

Lagrangian density:

$$\begin{aligned} \mathcal{L} = & \bar{\psi}_i \{i\gamma^\mu \partial_\mu - M\} \psi_i + \frac{1}{2} \partial^\mu \sigma \partial_\mu \sigma - U(\sigma) - g_\sigma \bar{\psi}_i \psi_i \sigma \\ & - \frac{1}{4} \Omega^{\mu\nu} \Omega_{\mu\nu} + \frac{1}{2} m_\omega^2 \omega^\mu \omega_\mu - g_\omega \bar{\psi}_i \gamma^\mu \psi_i \omega_\mu \\ & - \frac{1}{4} \vec{R}^{\mu\nu} \vec{R}_{\mu\nu} + \frac{1}{2} m_\rho^2 \vec{\rho}^\mu \vec{\rho}_\mu - g_\rho \bar{\psi}_i \gamma^\mu \vec{\tau} \psi_i \vec{\rho}_\mu \\ & - \frac{1}{4} F^{\mu\nu} F_{\mu\nu} - e \bar{\psi}_i \gamma^\mu \frac{1 - \tau_3}{2} \psi_i A_\mu \end{aligned}$$

The nonlinear potential of the sigma meson:

$$U(\sigma) = \frac{1}{2} m_\sigma^2 \sigma^2 + \frac{1}{3} g_2 \sigma^3 + \frac{1}{4} g_3 \sigma^4$$

The field tensors for the vector mesons and the photon are given as

$$\begin{aligned} \Omega^{\mu\nu} &= \partial^\mu \omega^\nu - \partial^\nu \omega^\mu, \\ \vec{R}^{\mu\nu} &= \partial^\mu \vec{\rho}^\nu - \partial^\nu \vec{\rho}^\mu - g_\rho (\vec{\rho}^\mu \times \vec{\rho}^\nu), \\ F^{\mu\nu} &= \partial^\mu A^\nu - \partial^\nu A^\mu. \end{aligned}$$

meson	J^π	T
π	0^-	1
σ	0^+	0
ω	1^-	0
ρ	1^-	1

Assumptions

- ★ **Static state assumption,**
- ★ **Time reversal symmetry, no currents, the spatial vector components vanish,**
- ★ **Charge conservation, only the 3-components of the isovector survives,**
- ★ **No sea approximation.**

The classical variational principle gives the Dirac equation for the nucleons and the Klein-Gordon equations for mesons and photon:

The Dirac equation for nucleons:

$$\{\boldsymbol{\alpha} \cdot \mathbf{p} + V(\mathbf{r}) + \beta(M + S(\mathbf{r}))\} \psi_i(\mathbf{r}) = \varepsilon_i \psi_i(\mathbf{r})$$

The corresponding density

$$\begin{aligned} \rho_s(\mathbf{r}) &= \sum_{i=1}^A \bar{\psi}_i(\mathbf{r}) \psi_i(\mathbf{r}) \\ \rho_v(\mathbf{r}) &= \sum_{i=1}^A \psi_i^\dagger(\mathbf{r}) \psi_i(\mathbf{r}) \\ \rho_3(\mathbf{r}) &= \sum_{i=1}^A \psi_i^\dagger(\mathbf{r}) \tau_3 \psi_i(\mathbf{r}) \\ \rho_p(\mathbf{r}) &= \sum_{i=1}^A \psi_i^\dagger(\mathbf{r}) \frac{1-\tau_3}{2} \psi_i(\mathbf{r}) \end{aligned}$$

The K-G equation for mesons and photon:

$$\begin{aligned} -\Delta \sigma(\mathbf{r}) + \partial_\sigma U(\sigma) &= -g_\sigma \rho_s(\mathbf{r}) \\ \{-\Delta + m_\omega^2\} \omega^0(\mathbf{r}) &= g_\omega \rho_v(\mathbf{r}) \\ \{-\Delta + m_\rho^2\} \rho^0(\mathbf{r}) &= g_\rho \rho_3(\mathbf{r}) \\ -\Delta A^0(\mathbf{r}) &= e \rho_p(\mathbf{r}) \end{aligned}$$

The vector and scalar potentials

$$\begin{aligned} V(\mathbf{r}) &= g_\omega \omega^0(\mathbf{r}) + g_\rho \tau_3 \rho_3^0(\mathbf{r}) + e \frac{1-\tau_3}{2} A^0(\mathbf{r}) \\ S(\mathbf{r}) &= g_\sigma \sigma(\mathbf{r}) \end{aligned}$$

These coupled equations are solved iteratively with the assumptions aforementioned. Then, we can obtain physical quantities on the properties of the nuclei.

Complex scaling method

The starting point of CSM is a coordinate transformation

$$\vec{r} \rightarrow \vec{r}' = g\vec{r} = e^{\Theta}\vec{r}$$

$g \in G$ (space dilation group), and Θ is of complex number.

Usually, Θ is adopted as a pure imaginary parameter $i\theta$ (θ is real)

The corresponding transformation operator $U(\theta)$ is defined as

$$[U(\theta)]\psi(\vec{r}) = e^{Ni\theta/2}\psi(\vec{r}e^{i\theta}) = \psi_{\theta}(\vec{r})$$

The transformed Hamiltonian

$$H_{\theta} = U(\theta)HU^{-1}(\theta)$$

The transformed equation of motion

$$H_{\theta}\psi_{\theta}(\vec{r}) = E_{\theta}\psi_{\theta}(\vec{r})$$

The transformation was introduced by Aguilar, Balslev, Combes and Simon.

ABC theorem

Conditions:

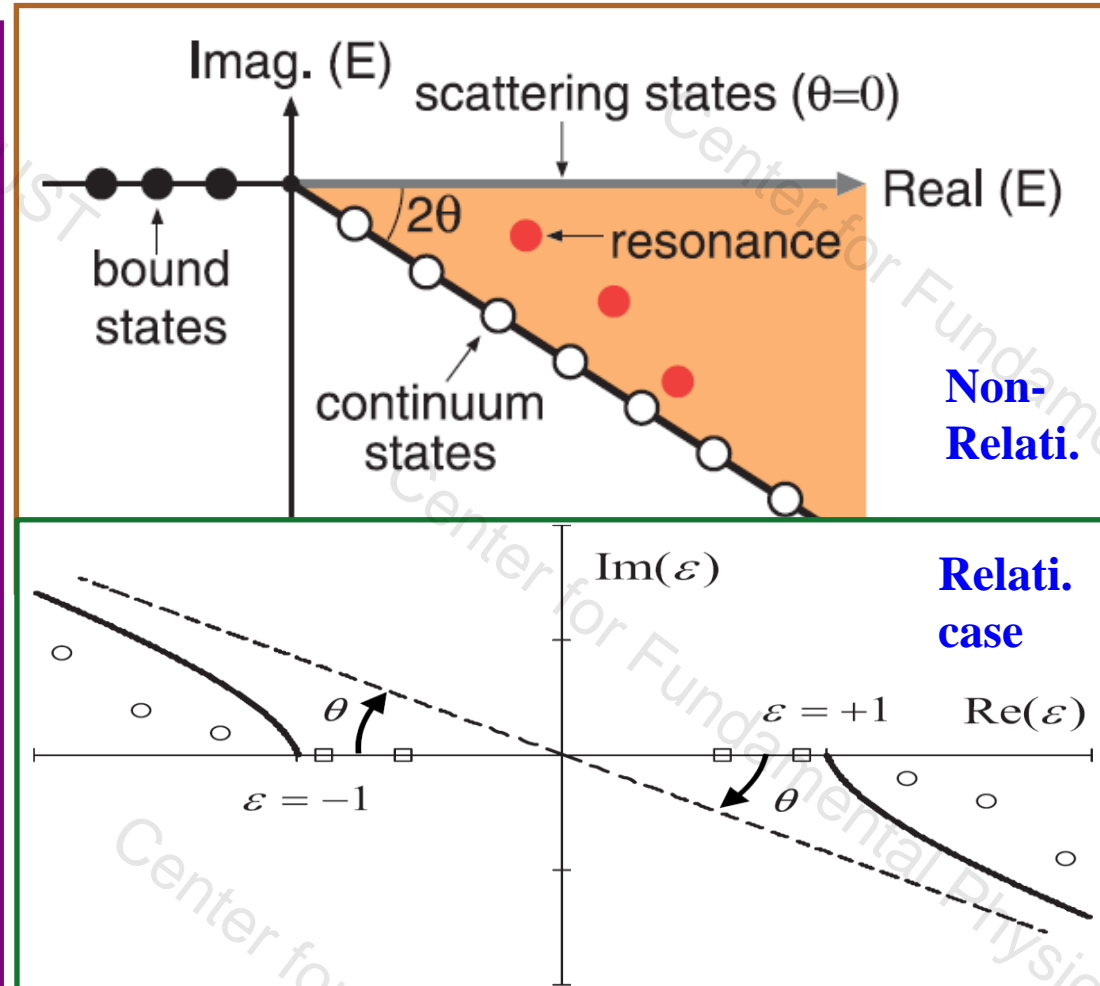
- The strongly restrictive sufficient conditions are given with mathematical rigor in the references above.
- loosely speaking they amount to the requirement that all quantities in the Schrödinger equation are **dilation analytic**.
- This means that there exists a finite region of θ in which their transforms obtained by the application of $U(\theta)$ are analytic.

J.Aguilar and J.M.Combes, Commun.Math.Phys.22,269(1971);
E.Balslev and J.M.Combes, ibid.22,280(1971); B.Simon, ibid.27,1(1972)

Results:

- A bound state eigenvalue of H remains also an eigenvalue of H_θ
- A resonance pole $E_{res} = E - i\Gamma/2$ of the Green-operator of H is an eigenvalue of H_θ
- The continuous part of the spectrum of H is rotated down into the complex energy plane by the angle 2θ .
- The important point is that the wavefunctions of resonant states are square integrable.

The solutions of H_θ in complex energy plane



Combined with RMF, the RMF-CSM formalism is established.

Neutron resonances in nuclei

PHYSICAL REVIEW C **82**, 034318 (2010)

Application of the complex scaling method in relativistic mean-field theory

Jian-You Guo, Xiang-Zheng Fang, Peng Jiao, Jing Wang, and Bao-Mei Yao

School of Physics and Material Science, Anhui University, Hefei 230039, People's Republic of China

(Received 9 October 2009; revised manuscript received 18 July 2010; published 21 September 2010)

We develop the complex scaling method within the framework of the relativistic mean-field (RMF) model. With the self-consistent nuclear potentials from the RMF model, the complex scaling method is used to study single-particle resonant states in spherical nuclei. As examples, the energies and widths of low-lying neutron resonant states in ^{120}Sn are obtained. The results are compared with those from the real stabilization method, the scattering phase-shift method, and the analytic continuation in the coupling constant approach and satisfactory agreements are found.

νl_j	RMF-CSM		RMF-RSM		RMF-ACCC		RMF-S	
	E	Γ	E	Γ	E	Γ	E	Γ
$\nu f_{5/2}$	0.67014	0.01982	0.674	0.030	0.685	0.023	0.688	0.032
$\nu i_{13/2}$	3.26583	0.00403	3.266	0.004	3.262	0.004	3.416	0.005
$\nu i_{11/2}$	9.59732	1.21178	9.559	1.205	9.60	1.11	10.01	1.42
$\nu j_{15/2}$	12.57745	0.99157	12.564	0.973	12.60	0.90	12.97	1.10

Proton resonances in nuclei

PHYSICAL REVIEW C **89**, 034307 (2014)

Probing single-proton resonances in nuclei by the complex-scaling method

Zhong-Lai Zhu, Zhong-Ming Niu,^{*} Dong-Peng Li, Quan Liu, and Jian-You Guo[†]

School of Physics and Material Science, Anhui University, Hefei 230601, China

(Received 15 January 2014; revised manuscript received 24 February 2014; published 12 March 2014)

By comparing the results of the complex-scaling method with those of the real-scaling method, we probe the influence of the complex-scaling method on the resonance energies and widths of the single-proton resonances in ^{132}Sn and ^{208}Pb . It is found that the complex-scaling method can provide more accurate results in the range of 0.4–0.6 MeV.

nl_j	RMF-CSM		RMF-ACCC		RMF-S	
	E_r	Γ	E_r	Γ	E_r	Γ
$2f_{7/2}$	6.207	0.048	6.22	0.073	6.210	0.043
$1h_{9/2}$	7.135	0.003	7.13	0.017	7.132	0.003
$3p_{3/2}$	7.305	0.911	7.32	0.82	7.513	0.924
$3p_{1/2}$	7.663	1.222	7.69	1.13	8.085	1.344
$2f_{5/2}$	7.919	0.283	7.97	0.30	7.934	0.307

Resonances are observed in the energy range of 0.4–0.6 MeV. In addition, the resonance energies and widths of the single-proton resonances in ^{132}Sn and ^{208}Pb are compared with those of the real-scaling method. It is found that the complex-scaling method can provide more accurate results in the range of 0.4–0.6 MeV.

RMF-CSM for deformed nuclei

PHYSICAL REVIEW C **86**, 054312 (2012)

Resonant states of deformed nuclei in the complex scaling method

Quan Liu, Jian-You Guo,^{*} Zhong-Ming Niu, and Shou-Wan Chen

School of Physics and Material Science, Anhui University, Hefei 230039, People's Republic of China

(Received 29 August 2012; revised manuscript received 14 October 2012; published 26 November 2012)

PHYSICAL REVIEW C **90**, 034319 (2014)

Relativistic extension of the complex scaling method for resonant states in deformed nuclei

Min Shi, Quan Liu, Zhong-Ming Niu, and Jian-You Guo^{*}

School of Physics and Material Science, Anhui University, Hefei 230601, People's Republic of China

(Received 3 August 2014; revised manuscript received 3 September 2014; published 24 September 2014)

The complex scaling method is extended to the relativistic framework for describing deformed nuclei and the theoretical formalism is presented in detail. How to expose the resonant states is demonstrated, and the applicability and efficiency of the extended method are confirmed. The energies and widths of the single-particle resonant states in nuclei with $A = 31$ are determined, and the structure of single-particle levels for bound and resonant states is shown to be similar to that in the nonrelativistic calculations. Especially, the present formalism has yielded richer numerical results for the resonant levels than those obtained by the coupled-channel method in relativistic and nonrelativistic calculations.

The RMF-CGF formalism

Complex scaled Green's function (CGF) method

Shi, Guo, et al.,
PRC92, 054313 (2015)

To more conveniently determine the resonance states, including the corresponding resonance parameters, we have developed a relativistic complex-scaled Green function method.

Complex scaled Green function is defined as

$$G^\theta(\varepsilon, \mathbf{r}, \mathbf{r}') = \langle \mathbf{r} | \frac{1}{\varepsilon - H_\theta} | \mathbf{r}' \rangle$$

where

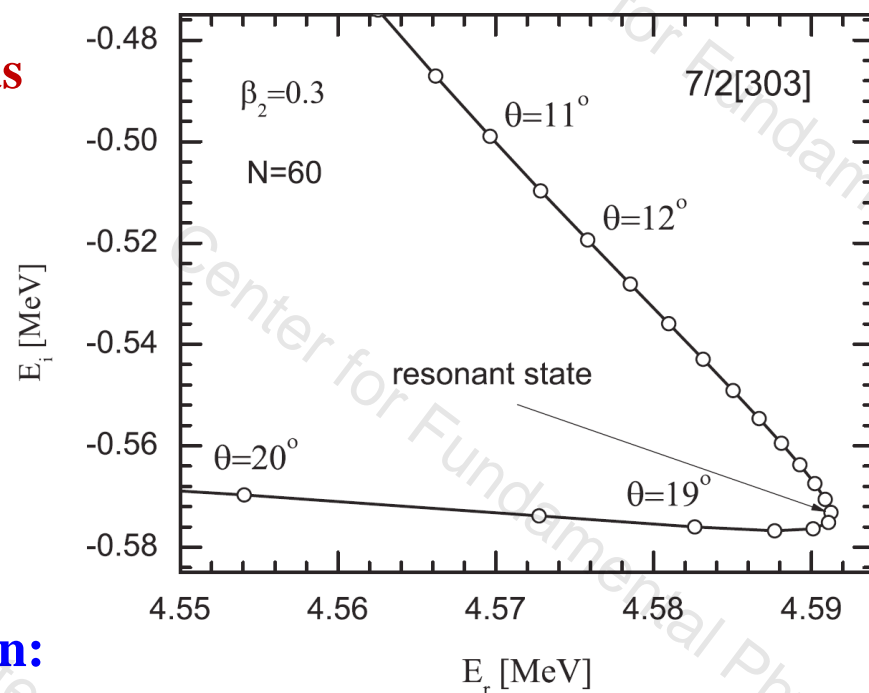
$$H_\theta = U(\theta) H U(\theta)^{-1},$$

The level density of system is defined as

$$\rho_\theta(\varepsilon) = -\frac{1}{\pi} \text{Im} \int d\mathbf{r} \langle \mathbf{r} | \frac{1}{\varepsilon - H_\theta} | \mathbf{r} \rangle$$

By using the extended completeness relation:

$$\sum_b^{N_b} |\psi_b^\theta\rangle \langle \tilde{\psi}_b^\theta| + \sum_r^{N_r} |\psi_r^\theta\rangle \langle \tilde{\psi}_r^\theta| + \int d\varepsilon_c^\theta |\psi_c^\theta\rangle \langle \tilde{\psi}_c^\theta| = 1,$$

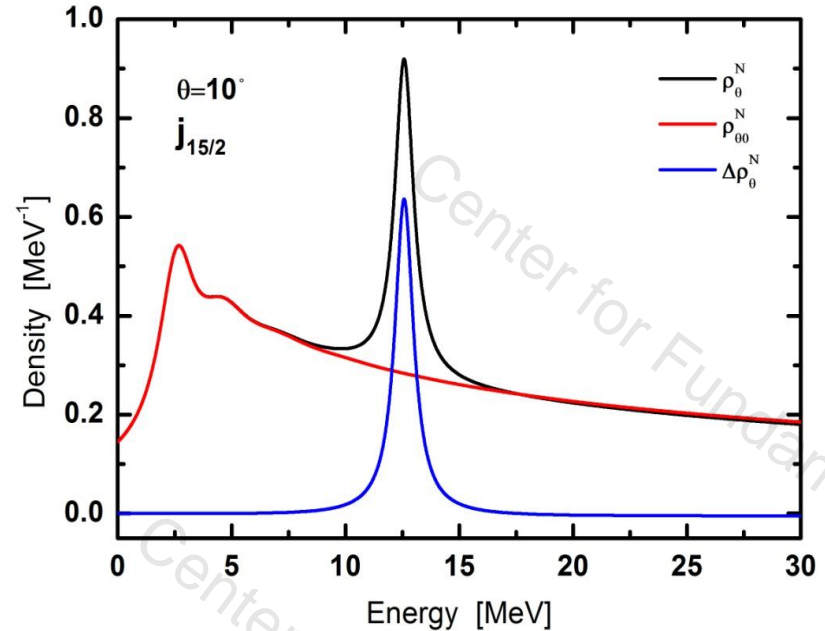


The level density is obtained as

$$\rho_{\theta}(\varepsilon) = -\frac{1}{\pi} \text{Im} \int d\mathbf{r} \left[\sum_b^{N_b} \frac{\psi_b^{\theta}(\mathbf{r}) \tilde{\psi}_b^{\theta*}(\mathbf{r})}{\varepsilon - \varepsilon_b} + \sum_r^{N_r} \frac{\psi_r^{\theta}(\mathbf{r}) \tilde{\psi}_r^{\theta*}(\mathbf{r})}{\varepsilon - \varepsilon_r^{\theta}} + \int d\varepsilon_c^{\theta} \frac{\psi_c^{\theta}(\mathbf{r}) \tilde{\psi}_c^{\theta*}(\mathbf{r})}{\varepsilon - \varepsilon_c^{\theta}} \right],$$

For the finite basis number N , the level density is expressed as

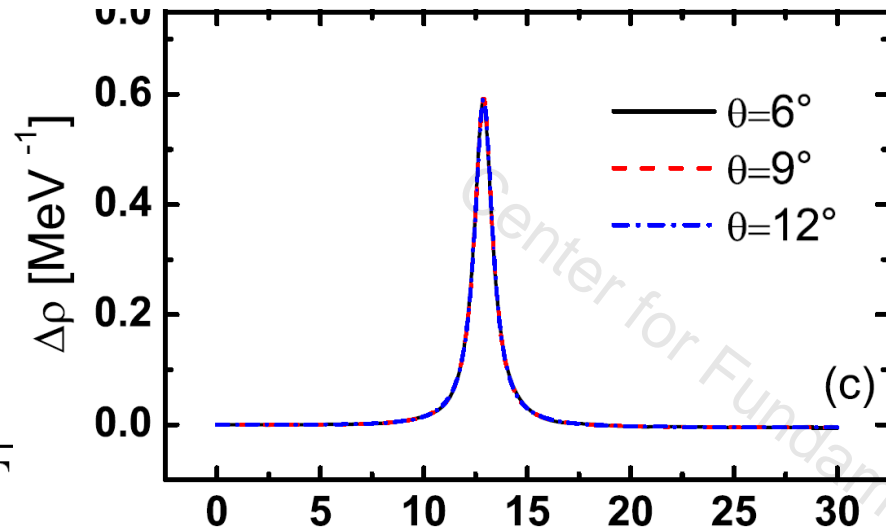
$$\rho_{\theta}^N(\varepsilon) = \sum_b^{N_b} \delta(\varepsilon - \varepsilon_b) + \frac{1}{\pi} \sum_r^{N_r} \frac{\Gamma_r/2}{(\varepsilon - E_r)^2 + \Gamma_r^2/4} + \frac{1}{\pi} \sum_c^{N-N_b-N_r} \frac{\varepsilon_c^I}{(\varepsilon - \varepsilon_c^R)^2 + \varepsilon_c^{I^2}}.$$



- The resonant state corresponds to the peak appearing in the density of energy level $\rho(\varepsilon)$.
- When θ is small, there exists oscillating phenomenon in $\rho(E)$.
- With the increasing of θ , the oscillating disappears.

The continuum level density is obtained by subtracting the background as

$$\begin{aligned} \Delta\rho(\varepsilon) &= \rho_{\theta}^N(\varepsilon) - \rho_{\theta}^{0N}(\varepsilon) \\ &= \sum_b^{N_b} \delta(\varepsilon - \varepsilon_b) + \frac{1}{\pi} \sum_r^{N_r} \frac{\Gamma_r/2}{(\varepsilon - E_r)^2 + \Gamma} \\ &\quad + \frac{1}{\pi} \sum_c^{N-N_b-N_r} \frac{\varepsilon_c^I}{(\varepsilon - \varepsilon_c^R)^2 + \varepsilon_c^{I^2}} \\ &\quad - \frac{1}{\pi} \sum_c^N \frac{\varepsilon_c^{0I}}{(\varepsilon - \varepsilon_c^{0R})^2 + \varepsilon_c^{0I^2}}, \end{aligned}$$



- When the background is removed off, the peak is more clear, which can be used accurately to determine the resonant parameters.
- The resonant state corresponds to the peak appearing in the density of energy level $\rho(\varepsilon)$.
- The dependence of θ disappears when θ is large.

Combined with RMF, the RMF-CGF formalism is established.

PHYSICAL REVIEW C **92**, 054313 (2015)

Relativistic extension of the complex scaled Green function method

Min Shi, Jian-You Guo,^{*} Quan Liu, Zhong-Ming Niu, and Tai-Hua Heng

School of Physics and Material Science, Anhui University, Hefei 230601, People's Republic of China

(Received 29 August 2015; revised manuscript received 23 October 2015; published 17 November 2015)

PHYSICAL REVIEW C **94**, 024302 (2016)

Probing resonances in deformed nuclei by using the complex-scaled Green's function method

Xin-Xing Shi, Min Shi, Zhong-Ming Niu, Tai-Hua Heng, and Jian-You Guo^{*}

School of Physics and Materials Science, Anhui University, Hefei 230601, People's Republic of China

(Received 29 May 2016; published 1 August 2016)

Resonance plays a key role in the formation of many physical phenomena. The complex-scaled Green's function method provides a powerful tool for exploring resonance. In this paper, we combine this method with the theory describing deformed nuclei with the formalism presented. Taking ^{45}S as an example, we elaborate numerical details and demonstrate how to determine the resonance parameters. The results are compared with those obtained by the complex scaling method and the coupled-channel method and satisfactory agreement is obtained. In particular, the present scheme focuses on the advantages of the complex scaling method and the Green's function method and is more suitable for the exploration of resonance.

There exist some shortcomings in CSM

- Need to introduce a unphysical parameter: complex rotation angle θ .
- CSM is only applicable to the dilation analytic potential.
- There is a singularity in the mean-field of nucleon movement when θ is very large. CSM is not applicable to very broad resonance in nuclei.



Complex momentum representation (CMR)

For the Woods-Saxon potential

$$V(r) = -\frac{V_0}{1 + \exp\left(\frac{r-R}{a}\right)}$$

Complex scaling transformation

$$V(re^{i\theta}) = -\frac{V_0}{1 + \exp\left(\frac{re^{i\theta}-R}{a}\right)}$$

When $\frac{re^{i\theta}-R}{a} = i\pi$, $\exp(i\pi) = -1$, $\tan\theta = \frac{\pi a}{R}$,

$V(re^{i\theta}) \rightarrow$ **singularity**

So, $\theta < \tan^{-1}\left(\frac{\pi a}{R}\right)$

When $R = 5 \text{ fm}$, $a = 0.6 \text{ fm}$, $\theta < 20.6^\circ$

The RMF-CMR formalism

Complex momentum representation (CMR)

In practical applications, it is more convenient to adopt the **momentum representation**

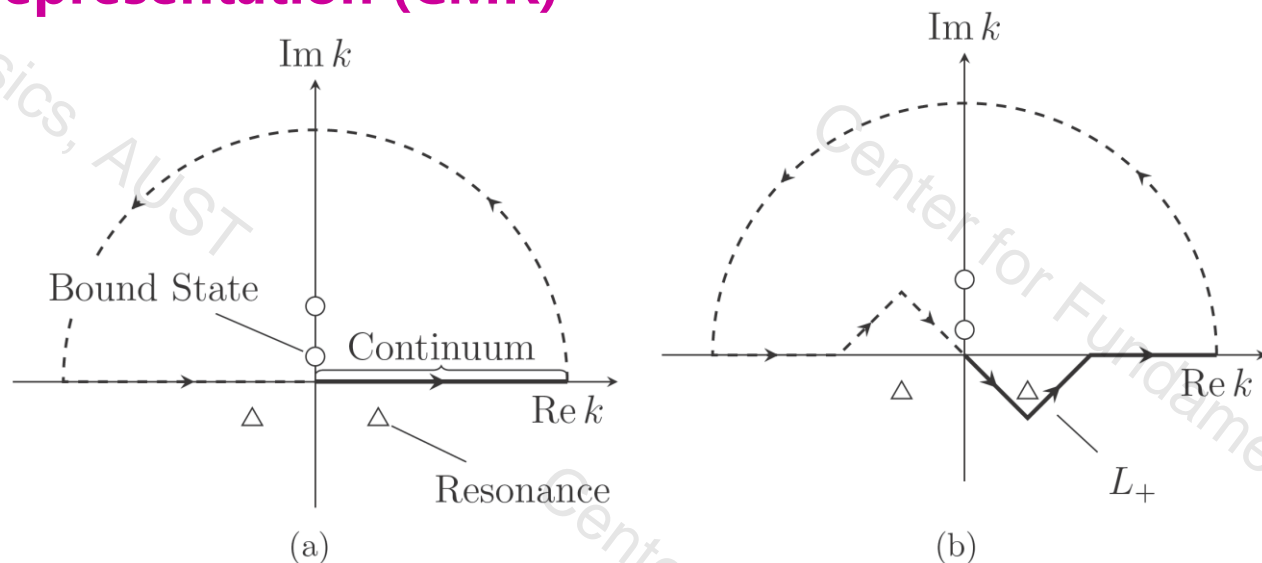
Completeness relation in momentum representation

$$\sum_{n \in (b,d)} |u_n\rangle \langle u_n| + \int_{L^+} |u(k)\rangle \langle u(k)| dk = 1$$

Orthogonality and Normalization relations

$$\langle \tilde{u}_2 | u_1 \rangle = 0 \quad \langle \tilde{u} | u \rangle = 1$$

where $\tilde{u} = u^*$ $\tilde{k} = -k^*$



- In real momentum space, we can only obtain bound states and scattering states.
- To obtain **resonant states**, **complex momentum representation is adopted.**

The Dirac equation is transformed into momentum representation:

Liu, Shi, Guo, et al.,
PRL117, 062502 (2016)

$$\int d\vec{k}' \langle \vec{k} | H | \vec{k}' \rangle \psi(\vec{k}') = \epsilon \psi(\vec{k})$$

where $H = \vec{\alpha} \cdot \vec{p} + \beta(M + S) + V$

For spherical nuclei

$$\psi(\vec{k}) = \begin{pmatrix} f(k) \phi_{l j m_j}(\Omega_k) \\ g(k) \phi_{\bar{l} j m_j}(\Omega_k) \end{pmatrix},$$

Dirac equation becomes

$$\begin{cases} M f(k) - k g(k) + \int k'^2 dk' V_+(k, k') f(k') = \epsilon f(k), \\ -k f(k) - M g(k) + \int k'^2 dk' V_-(k, k') g(k') = \epsilon g(k). \end{cases}$$

Here

$$V_+(k, k') = \frac{2}{\pi} \int r^2 dr [V(r) + S(r)] j_l(k'r) j_l(kr),$$

$$V_-(k, k') = \frac{2}{\pi} \int r^2 dr [V(r) - S(r)] j_{\bar{l}}(k'r) j_{\bar{l}}(kr).$$

For computational convenience, the equations are symmetricized and discretized as follows

$$\begin{cases} \sum_{b=1}^N \left[M\delta_{ab}\mathbf{f}(k_b) - k_a\delta_{ab}\mathbf{g}(k_b) + \sqrt{w_a w_b} k_a k_b V_+(k_a, k_b) \mathbf{f}(k_b) \right] = \varepsilon \mathbf{f}(k_a), \\ \sum_{b=1}^N \left[-k_a\delta_{ab}\mathbf{f}(k_b) - M\delta_{ab}\mathbf{g}(k_b) + \sqrt{w_a w_b} k_a k_b V_-(k_a, k_b) \mathbf{g}(k_b) \right] = \varepsilon \mathbf{g}(k_a). \end{cases}$$

where

$$\begin{cases} \mathbf{f}(k_a) = \sqrt{w_a} k_a f(k_a), \\ \mathbf{g}(k_a) = \sqrt{w_a} k_a g(k_a). \end{cases}$$

This set of equations is continued to complex momentum space, and its solutions include bound states, resonant states, and scattering states.

The normalization of wavefunction in complex momentum space

$$\int \tilde{\psi}(\vec{k}) \psi(\vec{k}) d\vec{k} = \sum_{a=1}^N [\mathbf{f}(k_a)\mathbf{f}(k_a) + \mathbf{g}(k_a)\mathbf{g}(k_a)]$$

Combined with RMF, the RMF-CMR formalism is established.

For deformed nuclei

The Dirac spinor is expanded as

$$\psi(\vec{k}) = \psi_{m_j}(\vec{k}) = \sum_{l'j'} \begin{pmatrix} f^{l'j'}(k)\phi_{l'j'm_j}(\Omega_k) \\ g^{l'j'}(k)\phi_{\tilde{l}'j'm_j}(\Omega_k) \end{pmatrix}, \quad (\tilde{l}' = 2j' - l')$$

Fang, Shi, Guo, Niu, Liang,
Zhang, PRC 95, 024311 (2017)

Dirac equation in momentum representation

$$\begin{cases} \sum_{b=1}^N \left[M\delta_{ab}\mathbf{f}^{lj}(k_b) + \sum_{l'j'} \sqrt{w_a w_b} k_a k_b V^+(l', j', p, q, l, j, m_j, k_a, k_b)\mathbf{f}^{l'j'}(k_b) - k_a \delta_{ab}\mathbf{g}^{lj}(k_b) \right] = \epsilon \mathbf{f}^{lj}(k_a), \\ \sum_{b=1}^N \left[-k_a \delta_{ab}\mathbf{f}^{lj}(k_b) - M\delta_{ab}\mathbf{g}^{lj}(k_b) + \sum_{l'j'} \sqrt{w_a w_b} k_a k_b V^-(\tilde{l}', j', p, q, \tilde{l}', j, m_j, k_a, k_b)\mathbf{g}^{l'j'}(k_b) \right] = \epsilon \mathbf{g}^{lj}(k_a) \end{cases}$$

where

$$\begin{aligned} & V^+(l', j', p, q, l, j, m_j, k, k') \\ &= (-)^l i^{l+l'} \frac{2}{\pi} \int r^2 dr [V(r) + S(r)] j_l(kr) j_{l'}(k'r) \sum_{m_s} \langle lm | Y_{pq}(\Omega_r) | l'm' \rangle \langle lm \frac{1}{2} m_s | jm_j \rangle \langle l'm' \frac{1}{2} m_s | j'm_j \rangle \\ & V^-(\tilde{l}', j', p, q, \tilde{l}', j, m_j, k, k') \\ &= (-)^{\tilde{l}'} i^{\tilde{l}'+\tilde{l}'} \frac{2}{\pi} \int r^2 dr [V(r) - S(r)] j_{\tilde{l}'}(kr) j_{\tilde{l}'}(k'r) \sum_{m_s} \langle \tilde{l}\tilde{m} | Y_{pq}(\Omega_r) | \tilde{l}'\tilde{m}' \rangle \langle \tilde{l}\tilde{m} \frac{1}{2} m_s | jm_j \rangle \langle \tilde{l}'\tilde{m}' \frac{1}{2} m_s | j'm_j \rangle \end{aligned}$$

The treatment of pairing correlations

Ding, Shi, Guo, Niu, Liang, PRC
98, 014316 (2018)

In the framework of RMF-CMR, the pairings are dealt with BCS approximation.

When the resonances are taken into account, the gap equation becomes

$$\sum_b \frac{\Omega_b}{\sqrt{(\varepsilon_b - \lambda)^2 + \Delta^2}} + \sum_r \Omega_r \int \frac{g_r(\varepsilon)}{\sqrt{(\varepsilon - \lambda)^2 + \Delta^2}} d\varepsilon = \frac{2}{G}$$

and the particle number equation

$$\sum_b \Omega_b \left[1 - \frac{\varepsilon_b - \lambda}{\sqrt{(\varepsilon_b - \lambda)^2 + \Delta^2}} \right] + \sum_r \Omega_r \int g_r(\varepsilon) \left[1 - \frac{\varepsilon - \lambda}{\sqrt{(\varepsilon - \lambda)^2 + \Delta^2}} \right] d\varepsilon = N$$

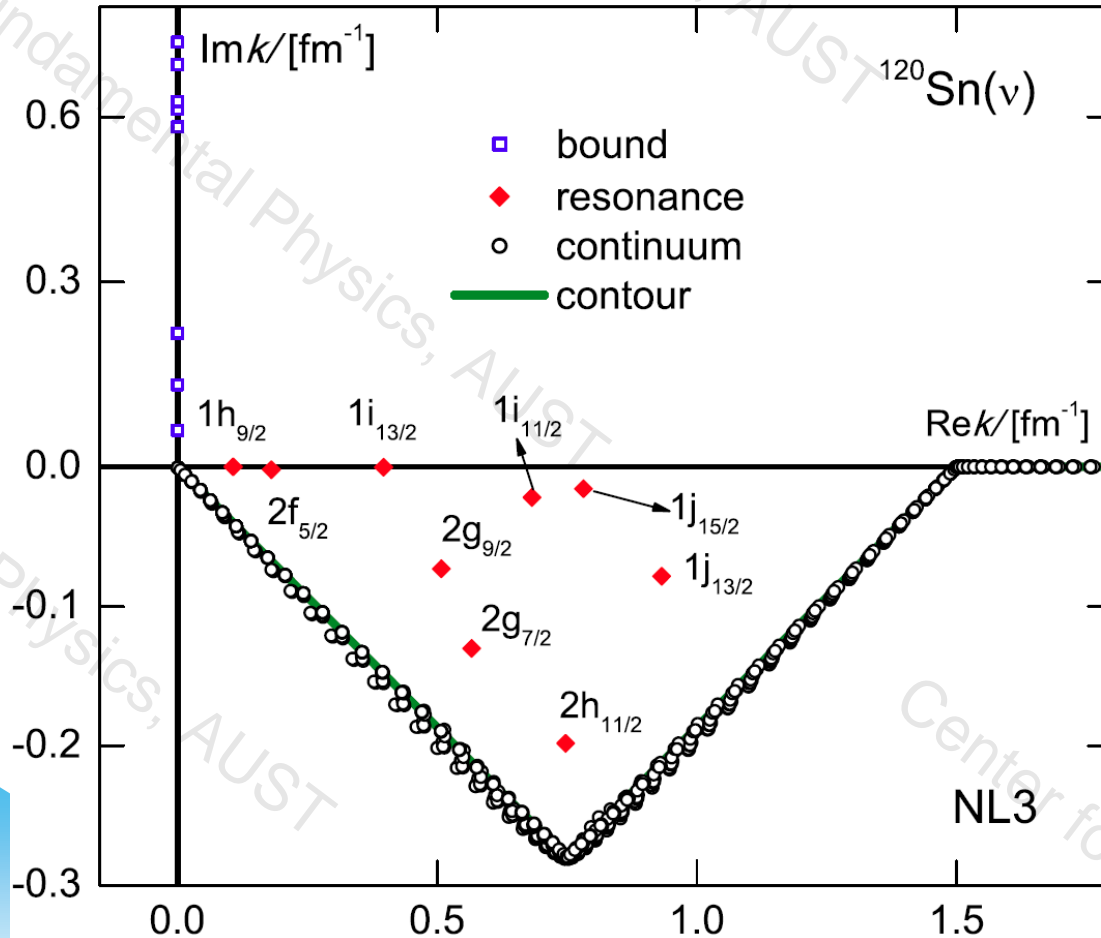
where

$$g_r(\varepsilon) = \frac{1}{\pi} \frac{\Gamma/2}{(\varepsilon - \varepsilon_r)^2 + \Gamma^2/4}$$

The RMF-CMR formalism 能够统一处理束缚态、共振态和散射态，能够描述稳定核，也能够描述远离稳定线弱束缚态的奇特结构与性质。

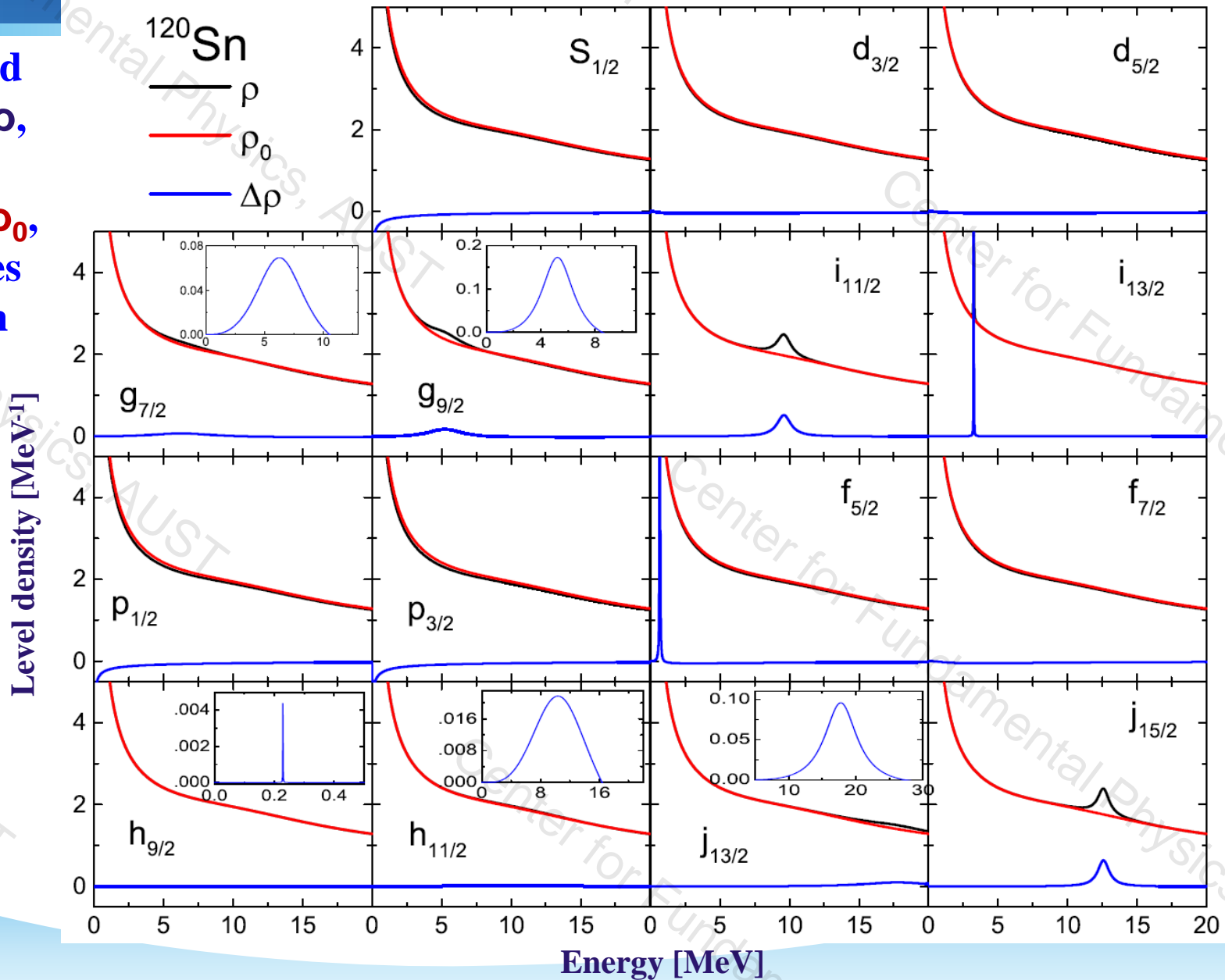
Exploration of neutron resonant states

Liu, Shi, Guo, et al.,
PRL117, 062502 (2016)



- CMR describes the bound states, resonant states, and continuum on an equal footing
- The bound states populate on the imaginary axis in the complex momentum plane
- The resonant states locate at the fourth quadrant
- The continuum follows the contour
- The bound states and resonant states are independent on the contour.

The calculated level density ρ , that from the background ρ_0 , the differences between them $\Delta\rho$.



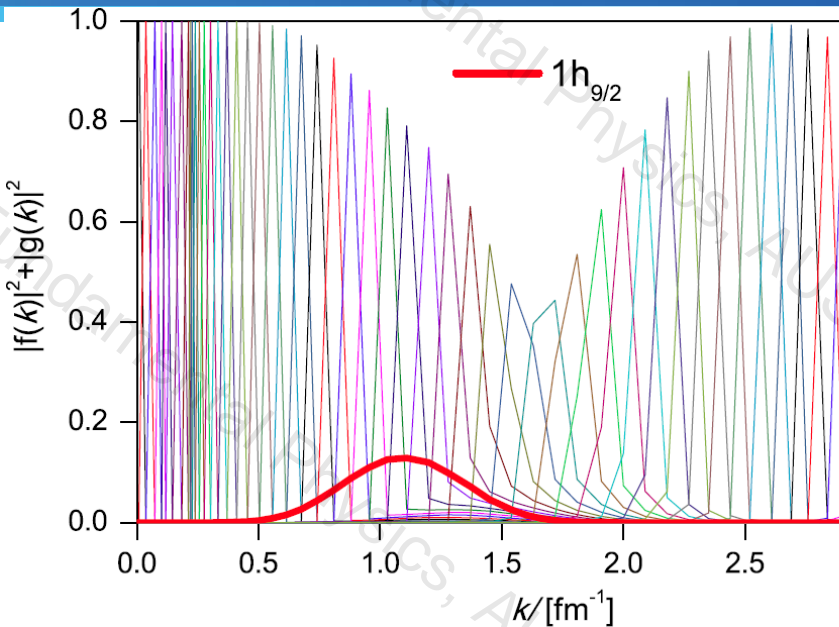


TABLE II. Energies and widths of single neutron resonant states for ^{120}Sn in the RMF-CMR calculations in comparison with the RMF-CSM, RMF-RSM, and RMF-ACCC calculations. Data are in units of MeV.

nl_j	RMF-CMR E_r, Γ	RMF-CSM E_r, Γ	RMF-RSM E_r, Γ	RMF-ACCC E_r, Γ
$2f_{5/2}$	0.678,0.031	0.670,0.020	0.674,0.030	0.685,0.023
$1i_{13/2}$	3.267,0.004	3.266,0.004	3.266,0.004	3.262,0.004
$1i_{11/2}$	9.607,1.219	9.597,1.212	9.559,1.205	9.60,1.11
$1j_{15/2}$	12.584,0.993	12.577,0.992	12.564,0.973	12.60,0.90

Wavefunction for the resonant state is expanded much wider than the free states which agrees the Heisenberg uncertainty principle: a less well defined momentum corresponds to a more well-defined position for bound and resonant states.

PRL **117**, 062502 (2016)

PHYSICAL REVIEW LETTERS

5 AUGUST 2016

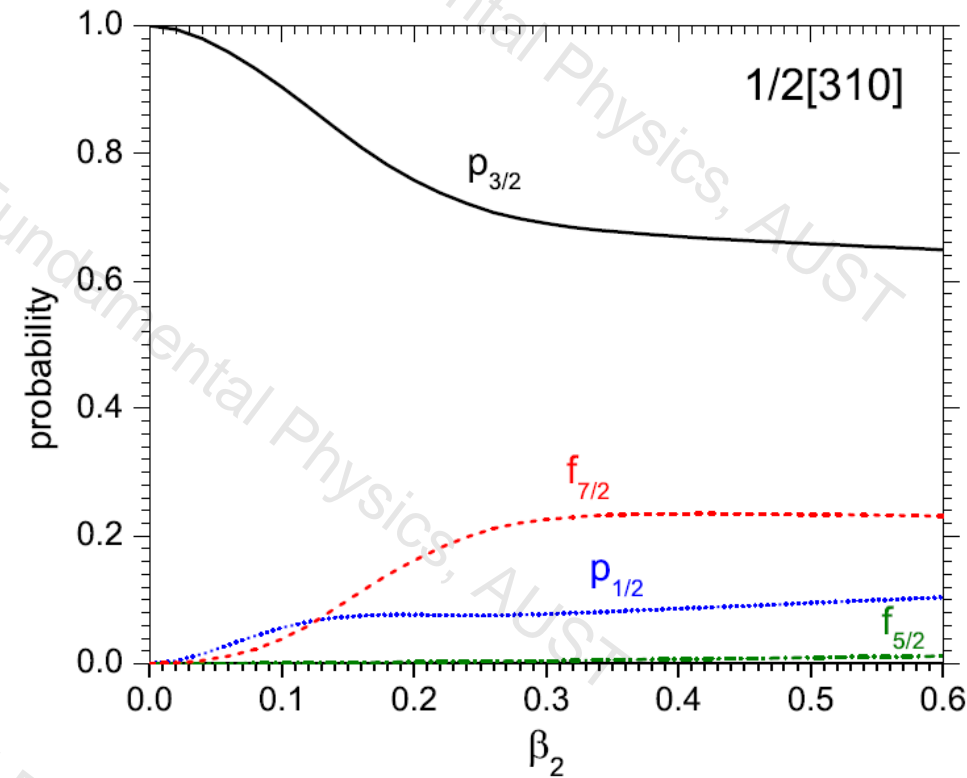
Probing Resonances of the Dirac Equation with Complex Momentum Representation

Niu Li (李牛),¹ Min Shi (仕敏),¹ Jian-You Guo (郭建友),^{1,*} Zhong-Ming Niu (牛中明),^{1,†} and Haozhao Liang (梁豪兆)^{2,3,‡}

¹School of Physics and Materials Science, Anhui University, Hefei 230601, People's Republic of China

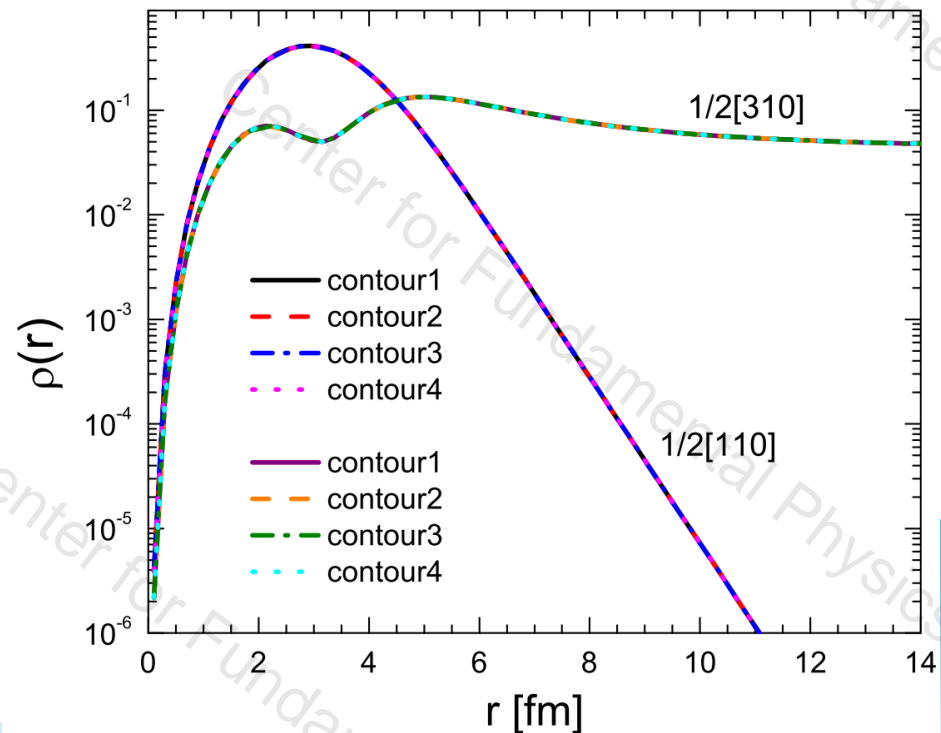
²RIKEN Nishina Center, Wako 351-0198, Japan

³Department of Physics, Graduate School of Science, The University of Tokyo, Tokyo 113-0033, Japan



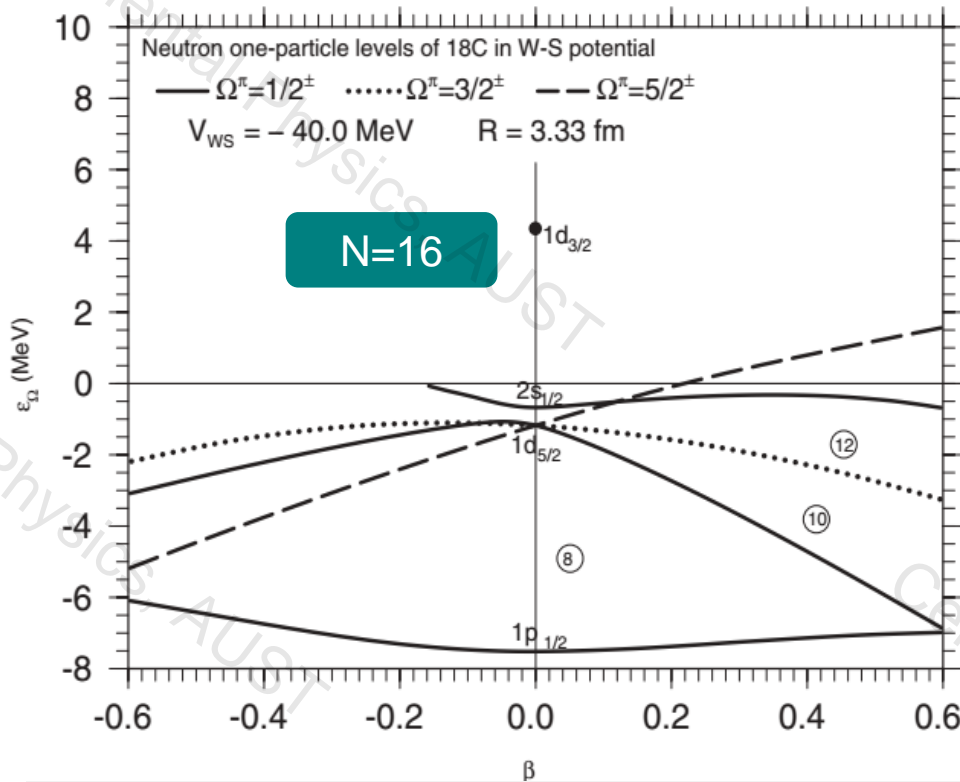
Density distributions of resonant states with a long tail.

Calculated probabilities of $p_{1/2}$, $p_{3/2}$, $f_{5/2}$, $f_{7/2}$, $h_{9/2}$, and $h_{11/2}$ components in the level 1/2[310]

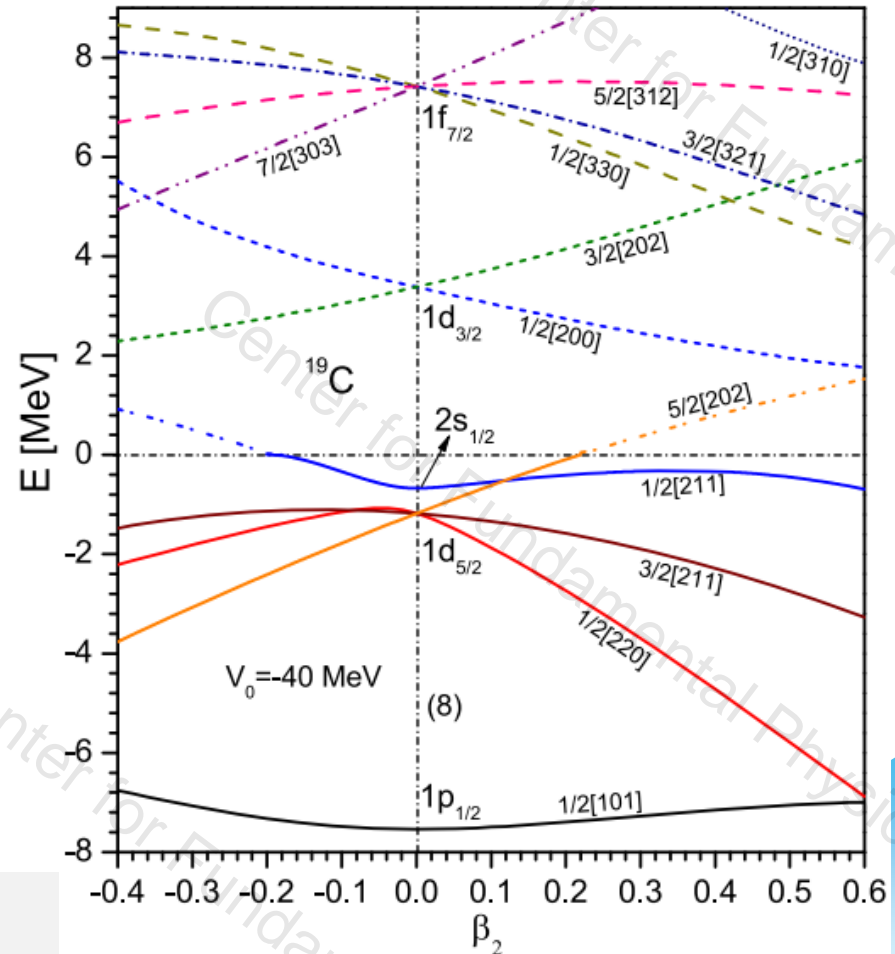


Neutron halo in ^{19}C

The single-particle energy levels of neutrons including the resonant levels in ^{19}C



X.N.Cao, Q.Liu, J.Y.Guo, JPG 45, 085105 (2018)



I. Hamamoto, PRC 85, 064329 (2012)

PHYSICAL REVIEW C **95**, 024311 (2017)

Probing resonances in the Dirac equation with quadrupole-deformed potentials with the complex momentum representation method

Zhi Fang,¹ Min Shi,^{1,2} Jian-You Guo,^{1,*} Zhong-Ming Niu,^{1,3} Haozhao Liang,^{2,3,4} and Shi-Sheng Zhang⁵

¹*School of Physics and Materials Science, Anhui University, Hefei 230601, People's Republic of China*

²*RIKEN Nishina Center, Wako 351-0198, Japan*

PHYSICAL REVIEW C **95**, 064329 (2017)

Research on the halo in ^{31}Ne with the complex momentum representation method

Ya-Juan Tian, Quan Liu,^{*} Tai-Hua Heng,[†] and Jian-You Guo[‡]

School of physics and materials science, Anhui University, Hefei 230601, People's Republic of China

(Received 14 April 2017; published 30 June 2017)

Interpretation of halo in ^{19}C with complex momentum representation method

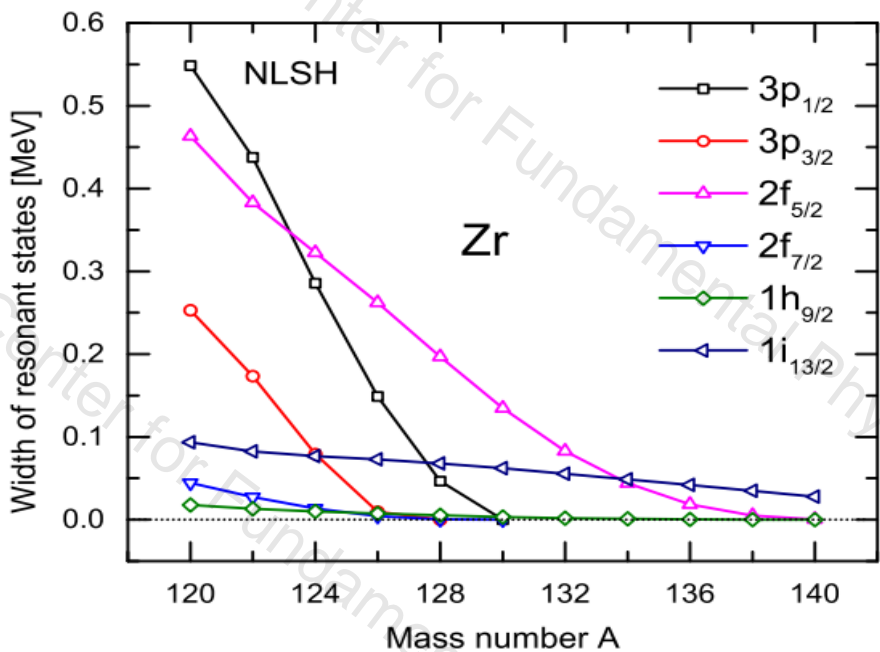
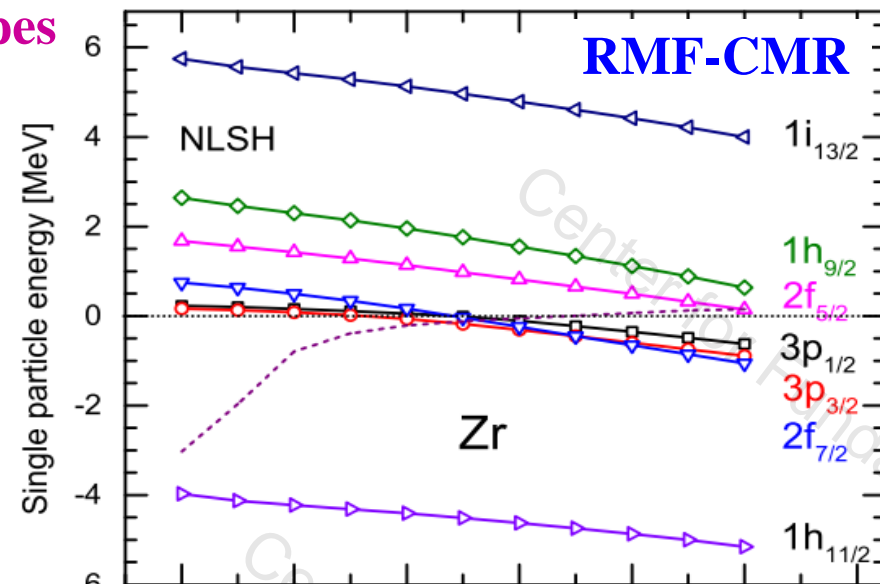
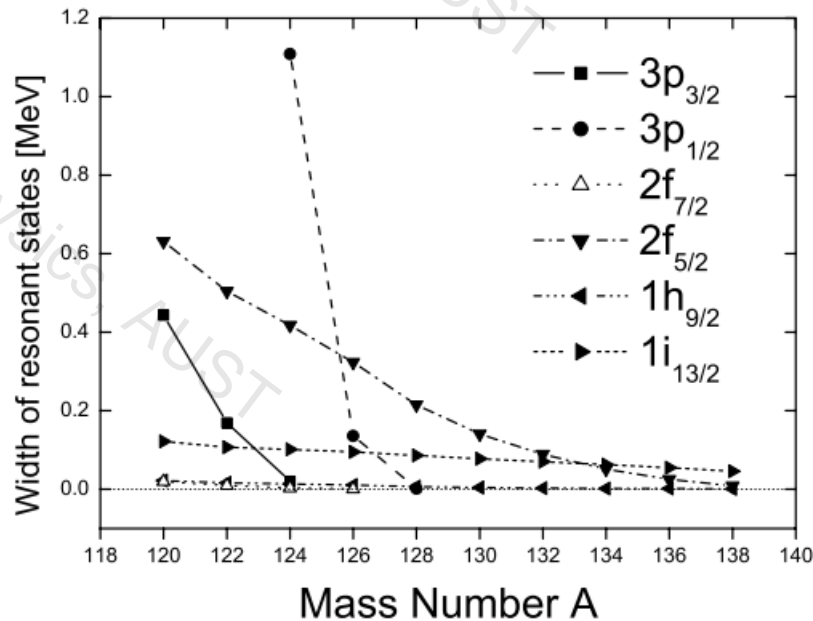
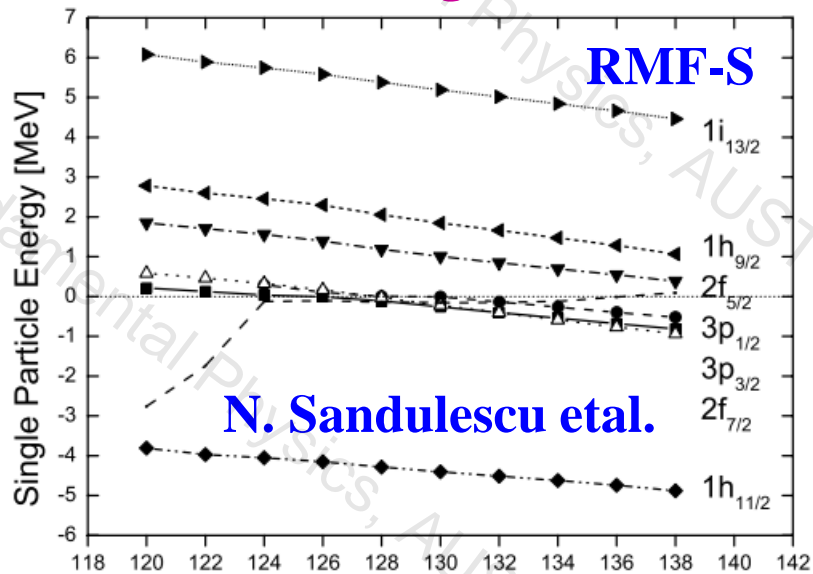
Xue-Neng Cao, Quan Liu¹  and Jian-You Guo

IOP Publishing

J. Phys. G: Nucl. Part. Phys. **45** (2018) 085105 (15pp)

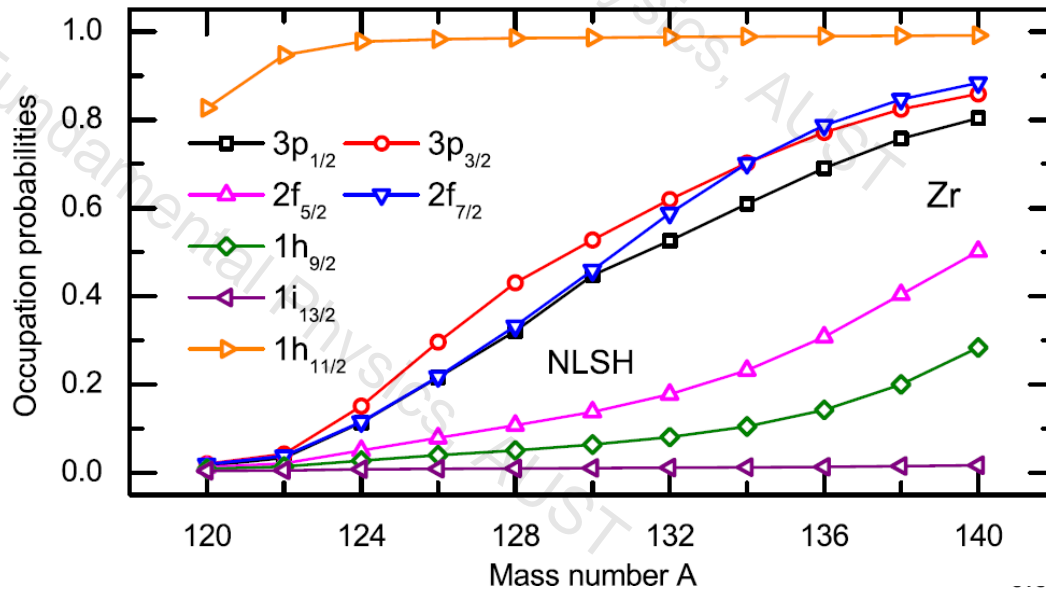
Predication on neutron halos

Neutron halo and giant halo Zr isotopes

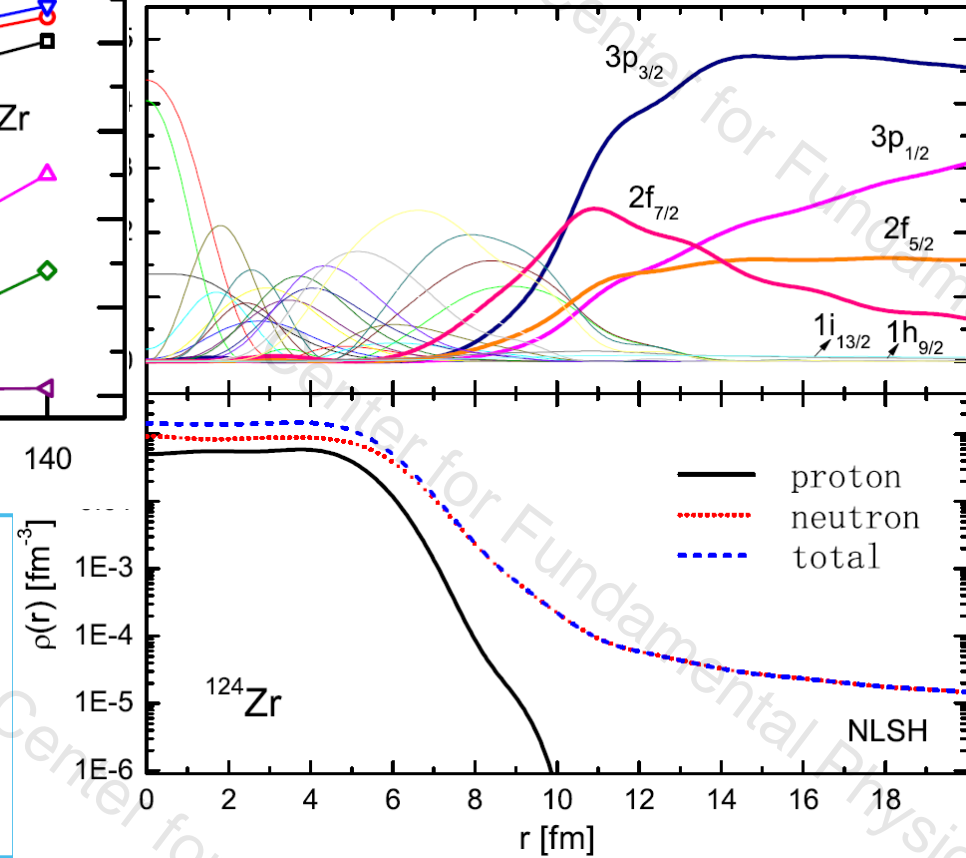


Occupation probabilities of neutron levels for the Zr isotopes

Ding, Shi, Guo, Niu, and Liang,
 PRC 98, 014316 (2018)



Density distributions in ^{124}Zr

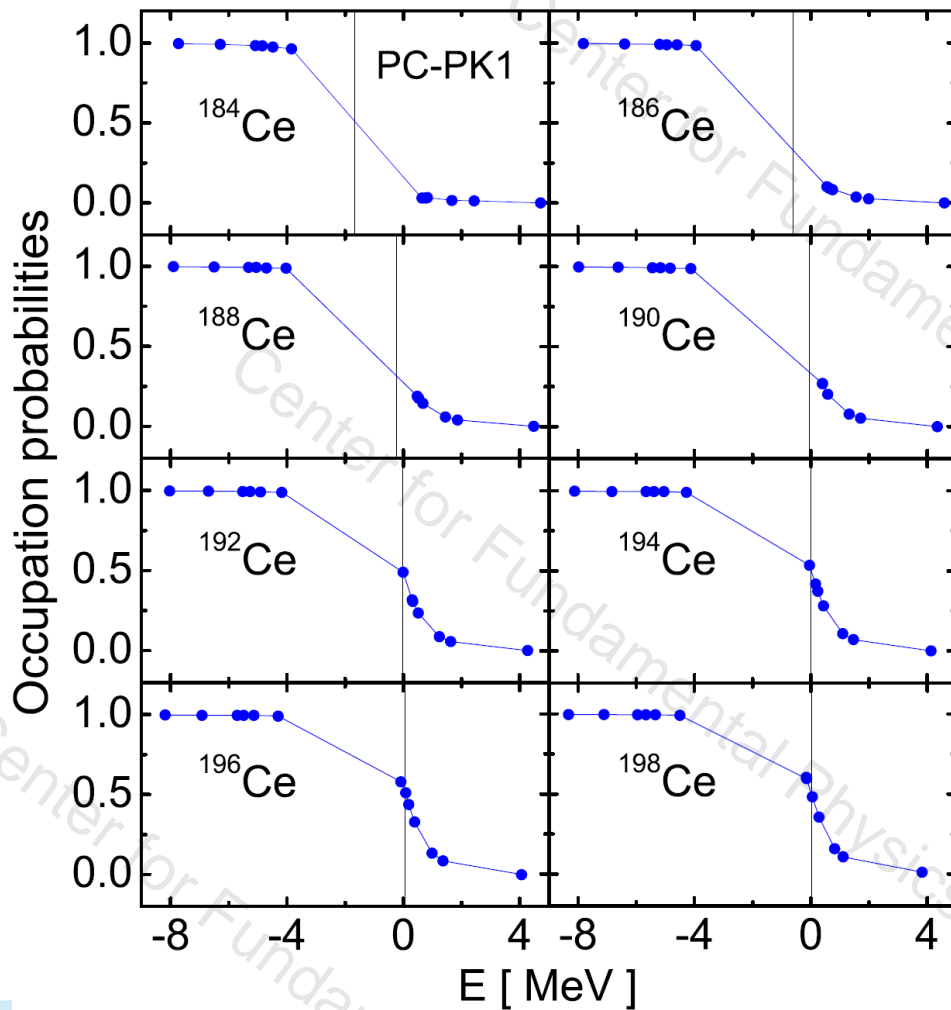
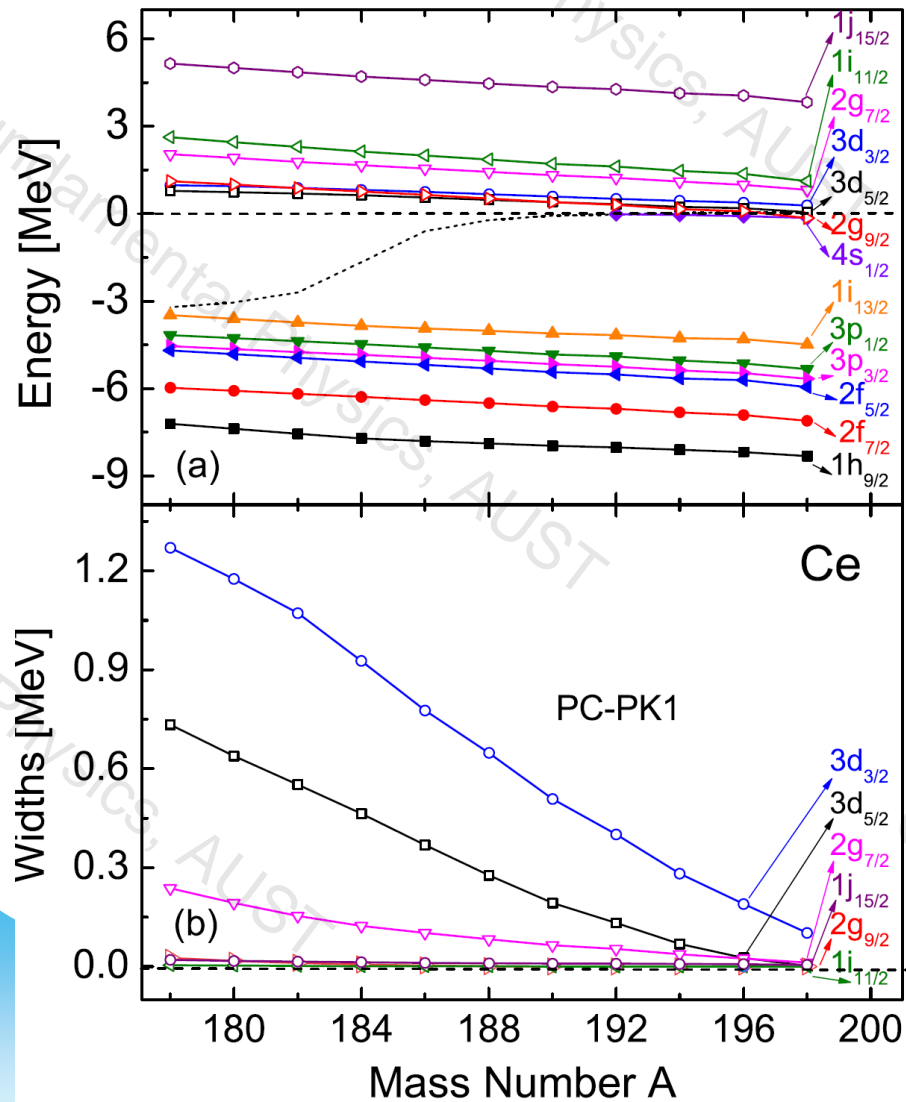


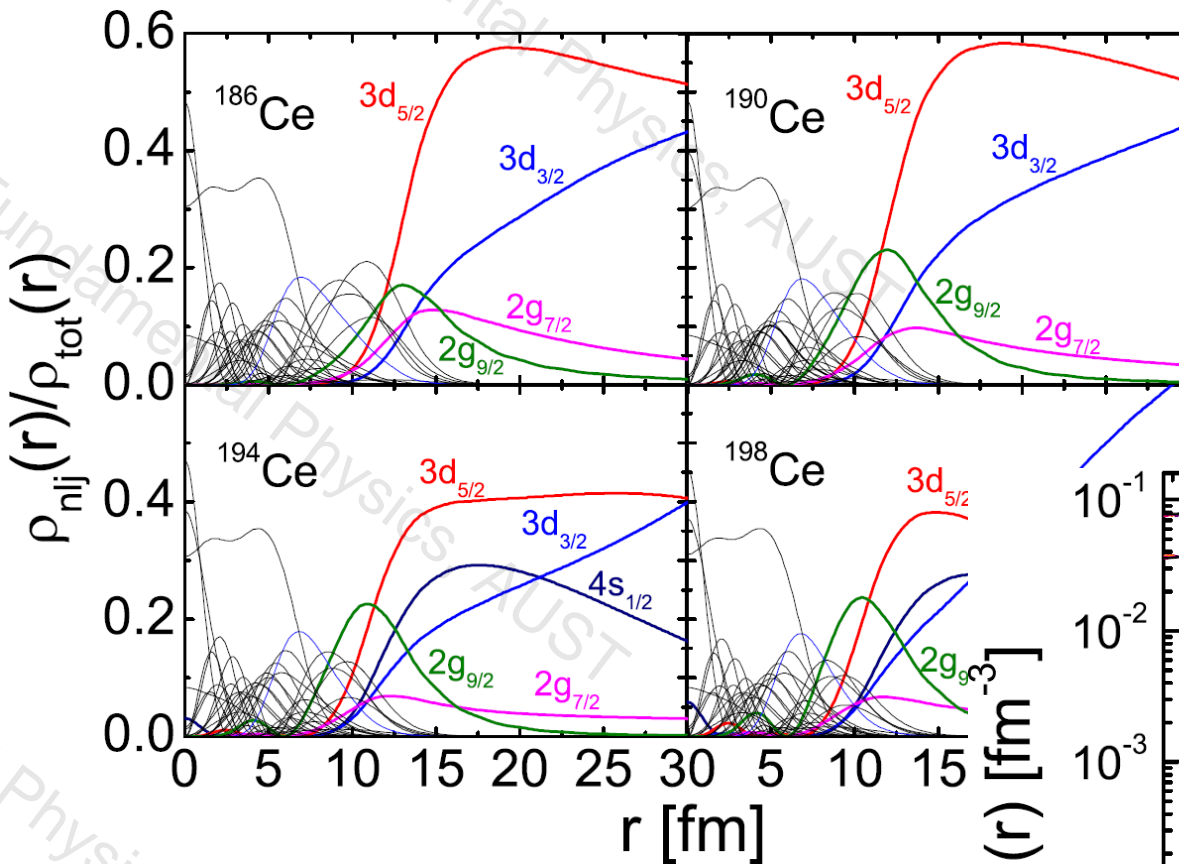
- The top panel displays the ratio of the neutron density of the single-particle levels to the total neutron density.
- The bottom panel displays the proton, neutron, and total matter densities.

➤ Neutron and matter density distributions in ^{124}Zr with a long tail, i.e., neutron halo appears in ^{124}Zr .

Neutron halo Ce isotopes

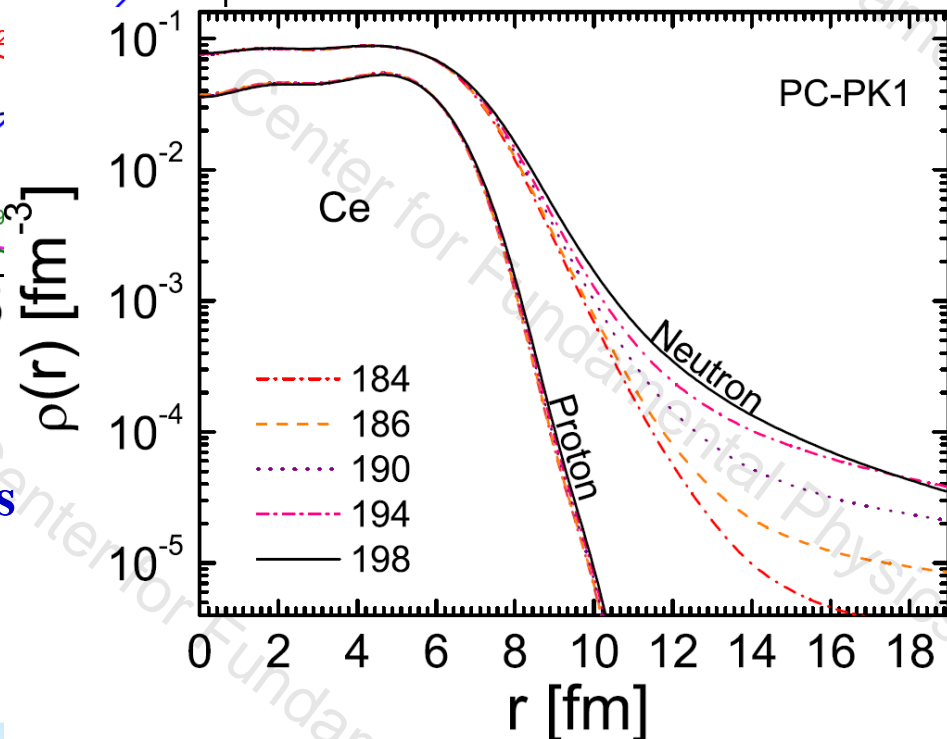
Cao, Ding, Shi, Liu, Guo,
 PRC 102, 044313 (2020)





The diffuse density distributions in $^{186-198}\text{Ce}$ come mainly from the contribution of the broad resonant states $3d_{5/2}$ and $3d_{3/2}$

The occupation number in halo orbits is more than two nucleons in $^{192-198}\text{Ce}$, which suggest that $^{186-190}\text{Ce}$ are halo nuclei and $^{192-198}\text{Ce}$ giant halo nuclei.

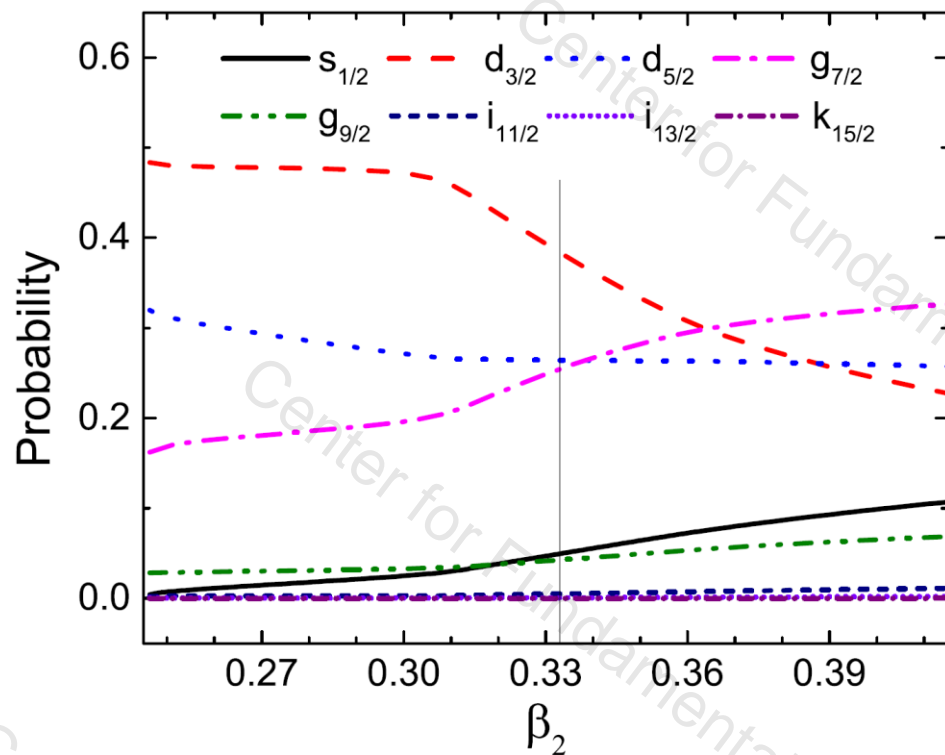
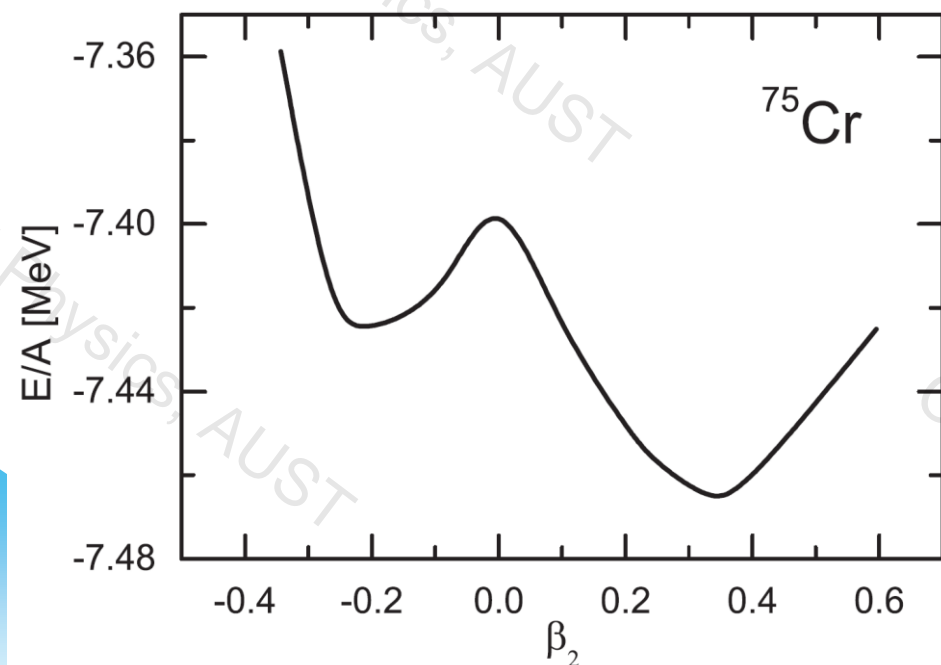


Deformed neutron halo ^{75}Cr , ^{77}Fe , ^{53}Ar

For example, ^{75}Cr

- 位能曲线显示基态形变 $\beta_2 \approx 0.333$;
- 最后的价中子占据 $1/2 [411]$

Cao, Liu, Guo, PRC 99, 014309 (2019);
Wang and Guo, PRC 104, 044315 (2021)

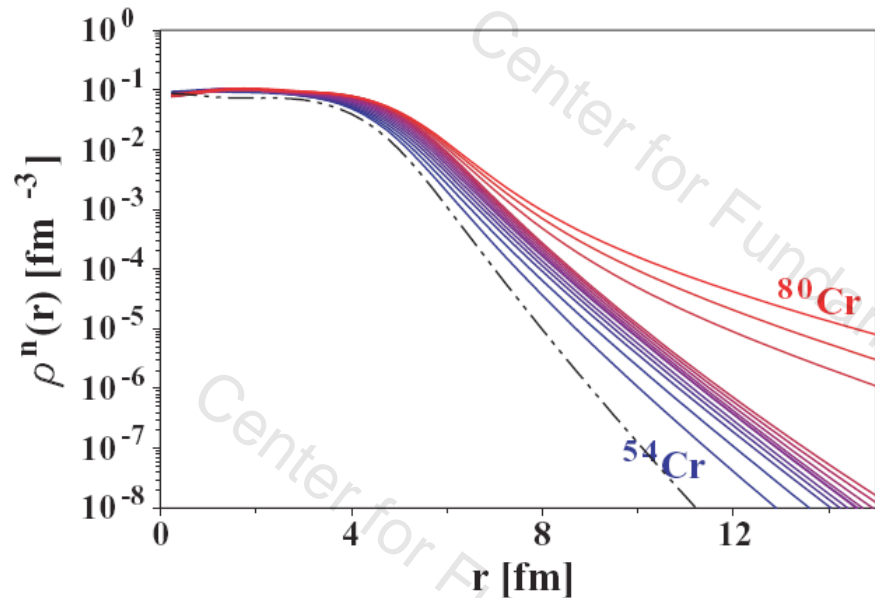
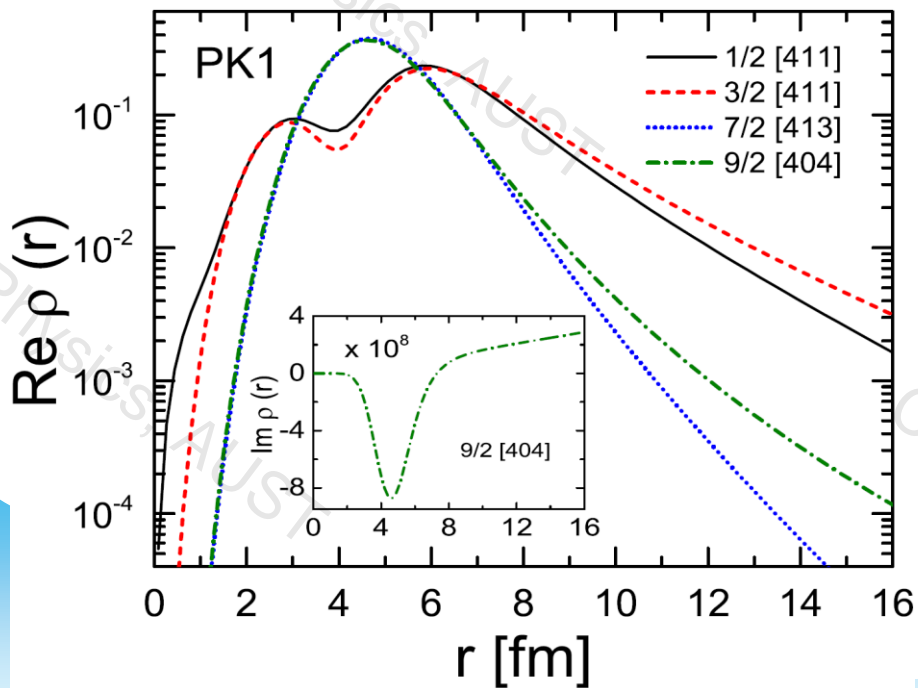


- 单粒子 $1/2 [411]$ 的组态占比;
- 在 $1/2 [411]$ 的组态构成中, 共振态 $d_{3/2}$ 占比近 40%

价核子轨道的密度分布:

SHFB calculation, V.Rotical, PRC 79, 054308 (2009)

- 最后价中子占据的 $1/2[411]$ 的密度分布是相当弥散的;
- $1/2[411]$ 主要由 $d_{3/2}$ 组态构成
- ^{75}Cr 是d-波晕核;

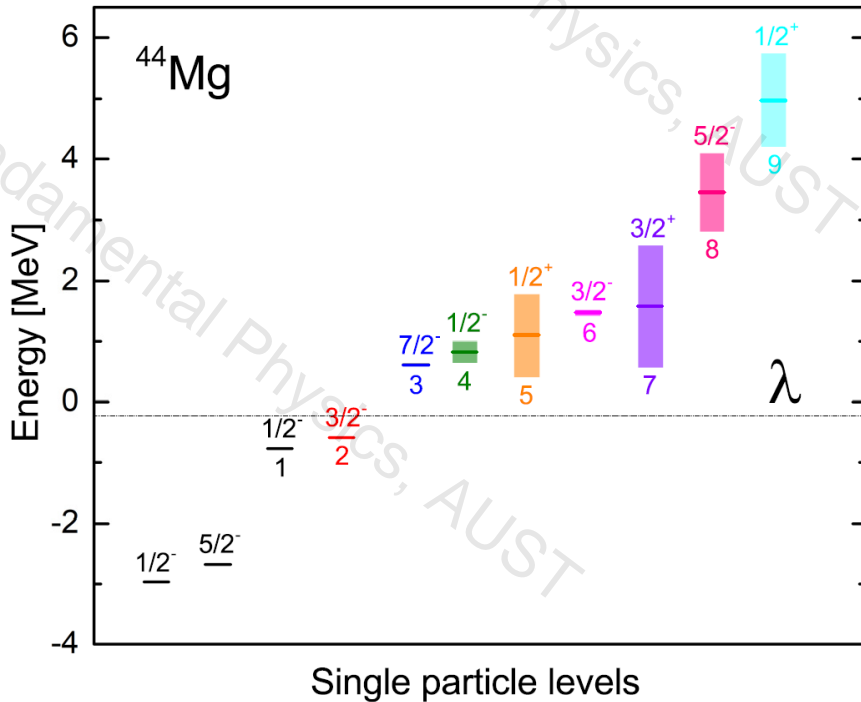


SHFB计算的价核子轨道的密度分布:

- $^{76,78,80}\text{Cr}$ 是中子晕核;
- 我们的结果和SHFB计算一致,
- 我们得出了 ^{75}Cr 是d-波晕核;

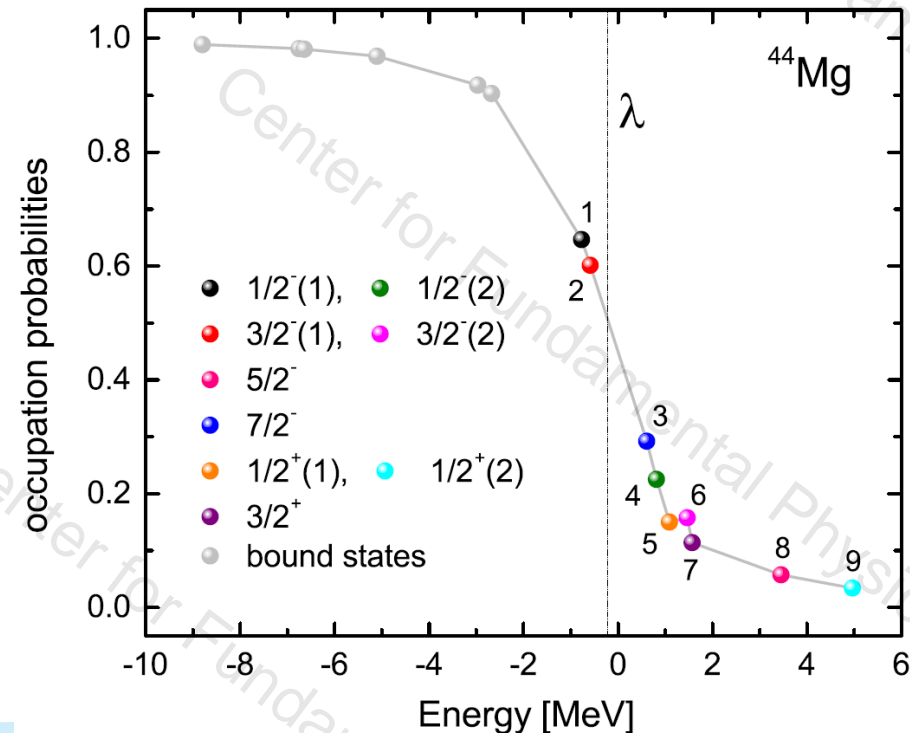
Deformed neutron halo in ^{44}Mg

Luo, Liu, Guo, PRC 108, 024320 (2023)

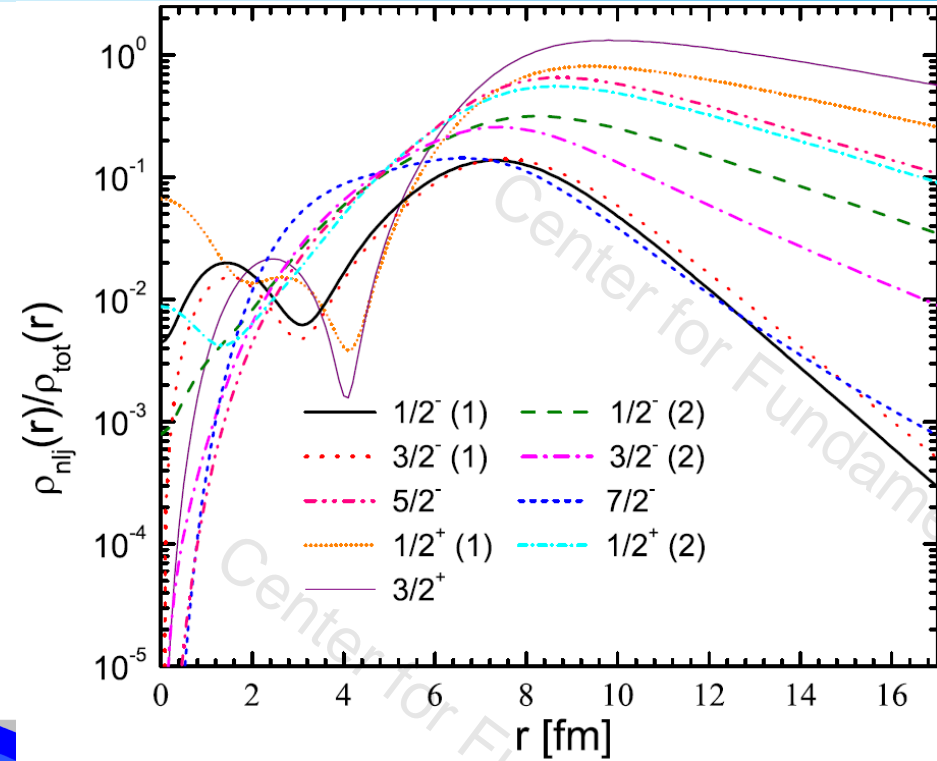
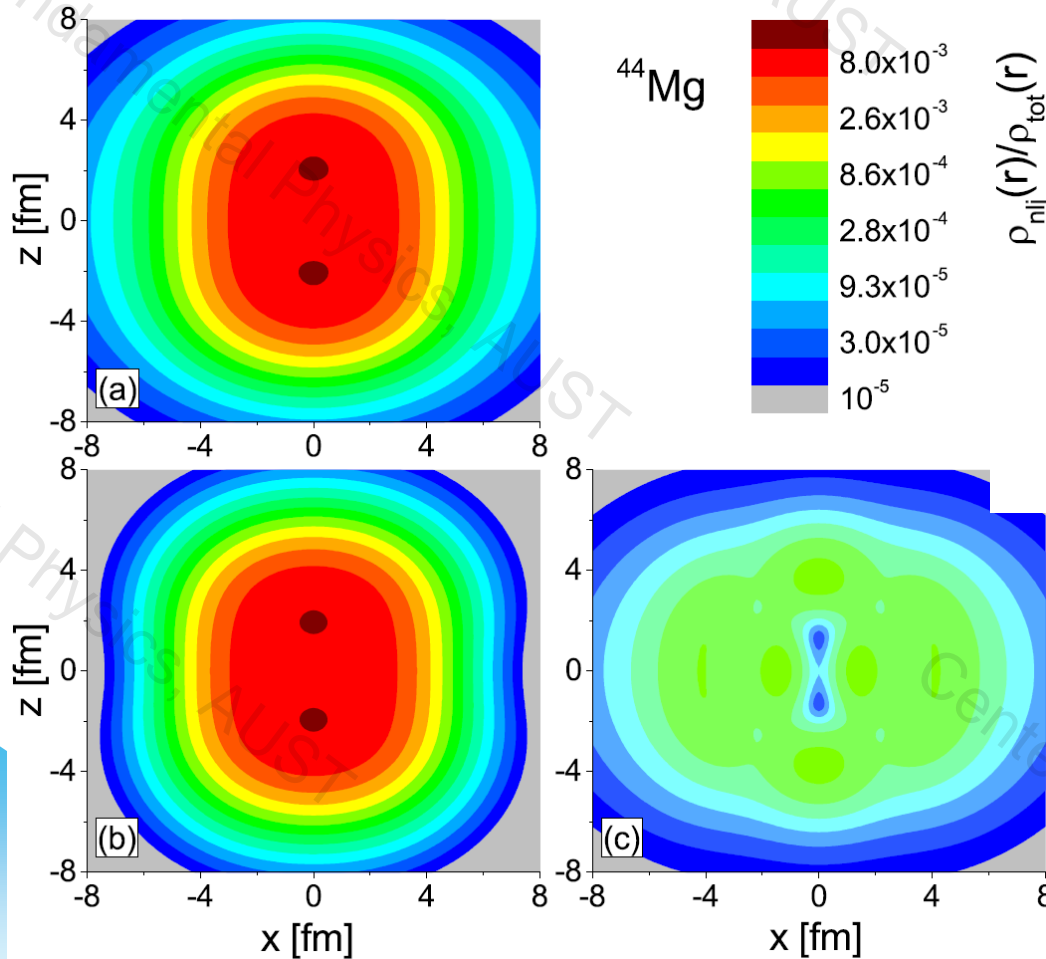


The single-neutron levels around Fermi surface including the bound states and resonant states in ^{44}Mg . The center line of the bar corresponds to the level position, and the height corresponds to the level width.

The occupation probabilities of single particle levels around Fermi surface in ^{44}Mg . The relatively bound levels are denoted as gray circles. The weakly bound and resonant levels are marked as solid circles.



(a) Total neutron density distributions,
 (b) that from the deeply bound levels,
 (c) from the weakly bound and resonant levels.



The ratios of the density distributions of single particle levels to the total density distributions for the weakly bound and resonant levels in ^{44}Mg for neutrons.

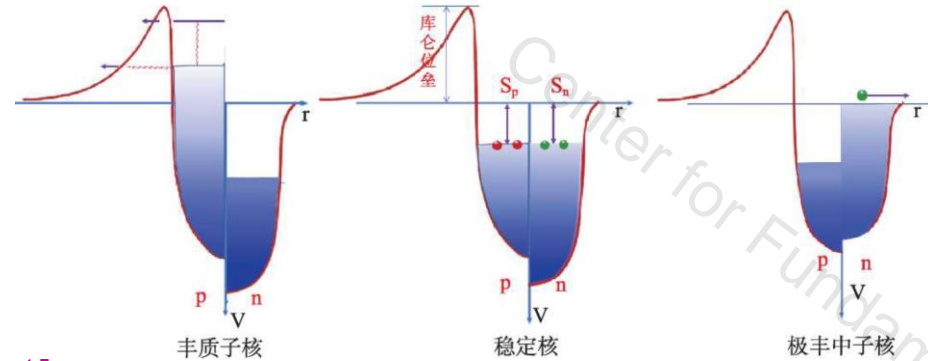
RMF-CMR for proton

Different from the case of neutron, there is the singularity in the Dirac equation in momentum representation for Coulomb field.

靳根明 现代物理知识杂志 2023-12-11

Without losing generality, a screening coulomb potential is considered•

$$V_c(\vec{r}) = \lambda \frac{\exp(-\eta r)}{r}$$



Dirac equation in momentum representations

$$\begin{cases} Mf(k) - kg(k) + \int k'^2 dk' V_c^l(k, k') f(k') = \varepsilon f(k), \\ -kf(k) - Mg(k) + \int k'^2 dk' V_c^{\tilde{l}}(k, k') g(k') = \varepsilon g(k), \end{cases}$$

Where

$$V_c^l(k, k') = \frac{\lambda}{\pi} \frac{Q_l(y)}{kk'}, \quad V_c^{\tilde{l}}(k, k') = \frac{\lambda}{\pi} \frac{Q_{\tilde{l}}(y)}{kk'}. \quad y = \frac{k^2 + k'^2 + \eta^2}{2kk'}$$

Because $Q_l(y) = P_l(y)Q_0(y) - W_{l-1}(y)$ $W_{l-1}(y) = \sum_{i=1}^l \frac{1}{i} P_{l-i}(y) P_{i-1}(y)$

$$Q_0(y) = \frac{1}{2} \ln \frac{y+1}{y-1}$$

When $\eta \rightarrow 0$ $k' = k$ $y = 1$

There is the singularity in Q_l and $Q_{\tilde{l}}$,

To eliminate the singularity, Lande subtraction is adopted. The integral in Dirac equation is separated into the two parts:

$$\int_0^{\infty} V_c^l(k, k') f_l(k') k'^2 dk' = A + B,$$

where

$$A = \int_0^{\infty} V_c^l(k, k') \left[f_l(k') k'^2 - \frac{f_l(k) k^2}{P_l(y)} \right] dk',$$

$$B = f_l(k) k^2 \int_0^{\infty} \frac{V_c^l(k, k')}{P_l(y)} dk'.$$

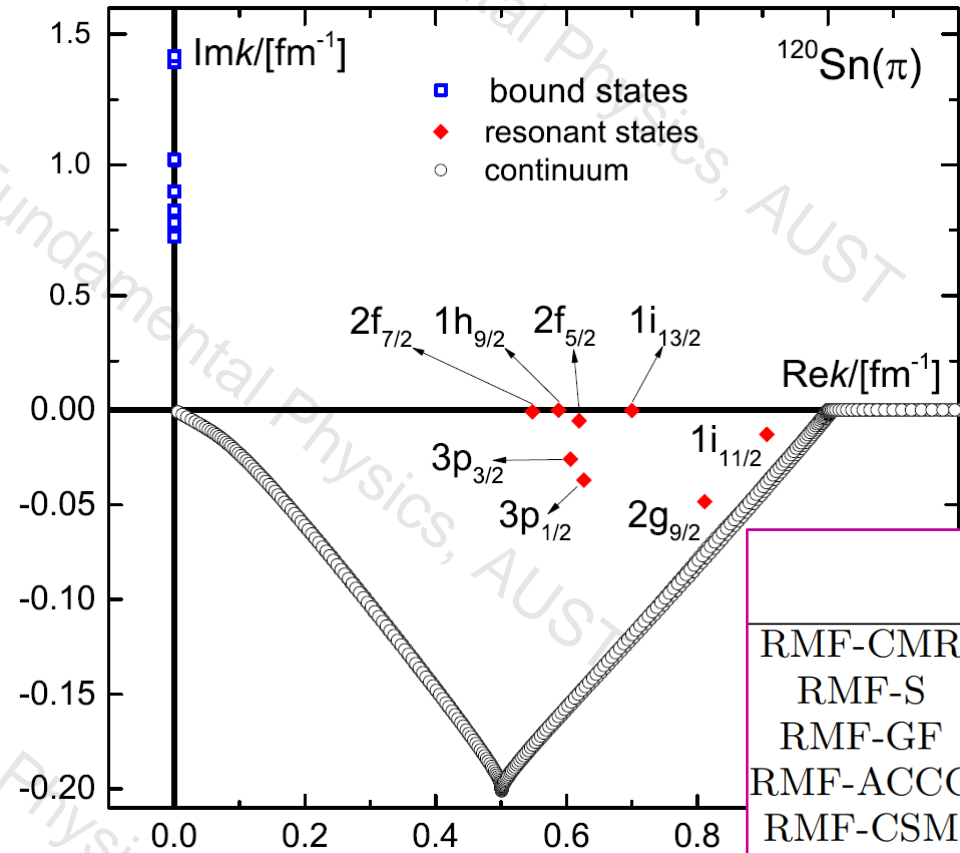
The integral in A can be set with $k \neq k'$ because $A = 0$ with $k = k'$.

The integral in B can be calculated as:

$$\int_0^{\infty} \frac{V_c^l(k, k')}{P_l(y)} dk' = \frac{\lambda}{\pi k} \int_0^{\infty} \frac{Q_l(y)}{P_l(y)} \frac{dk'}{k'} = \frac{\lambda}{k} \left(\frac{\pi}{2} - I_l \right)$$

I_l can be evaluated exactly, $I_0 = 0$, $I_1 = 1$, $I_2 = 1.2247448713915894, \dots$

Exploration of proton resonant states



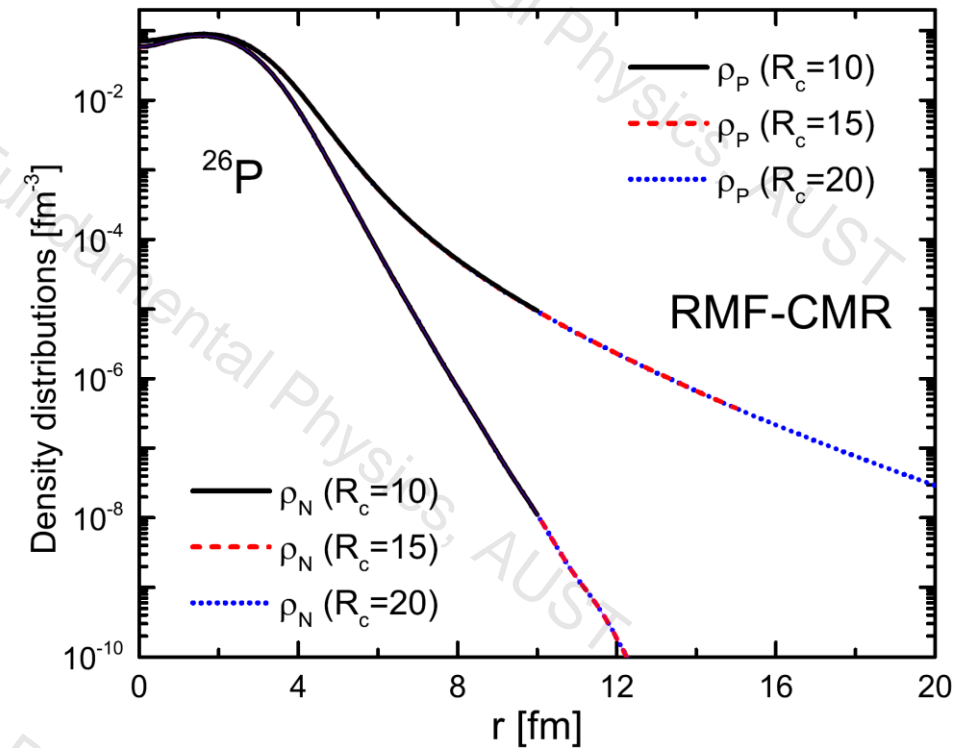
- Singularity of long-range Coulomb potential is eliminated in the RMF-CMR calculations.
- All these results from the five different methods are comparable.
- Our calculations match better the scattering phase shift calculations.

	$2f_{7/2}$ E, Γ	$1h_{9/2}$ E, Γ	$3p_{3/2}$ E, Γ	$2f_{5/2}$ E, Γ
RMF-CMR	6.210,0.042	7.133,0.003	7.567,1.291	7.917,0.294
RMF-S	6.210,0.043	7.132,0.003	7.513,0.924	7.934,0.307
RMF-GF	6.205,0.037	7.134,0.002	7.265,0.965	7.909,0.365
RMF-ACCC	6.220,0.073	7.130,0.017	7.320,0.820	7.970,0.300
RMF-CSM	6.207,0.048	7.135,0.003	7.305,0.911	7.919,0.282
	$3p_{1/2}$ E, Γ	$1i_{13/2}$ E, Γ	$2g_{9/2}$ E, Γ	$1i_{11/2}$ E, Γ
RMF-CMR	8.166,2.052	10.110,0.012	13.510,3.208	16.889,0.946
RMF-S	8.085,1.344	10.110,0.012		16.960,0.999
RMF-GF	7.667,1.233	10.110,0.014		16.934,1.092
RMF-ACCC	7.690,1.130			
RMF-CSM	7.663,1.222			

$$V_c^l(k, k') = \frac{\lambda}{\pi} \frac{Q_l(y)}{kk'}$$

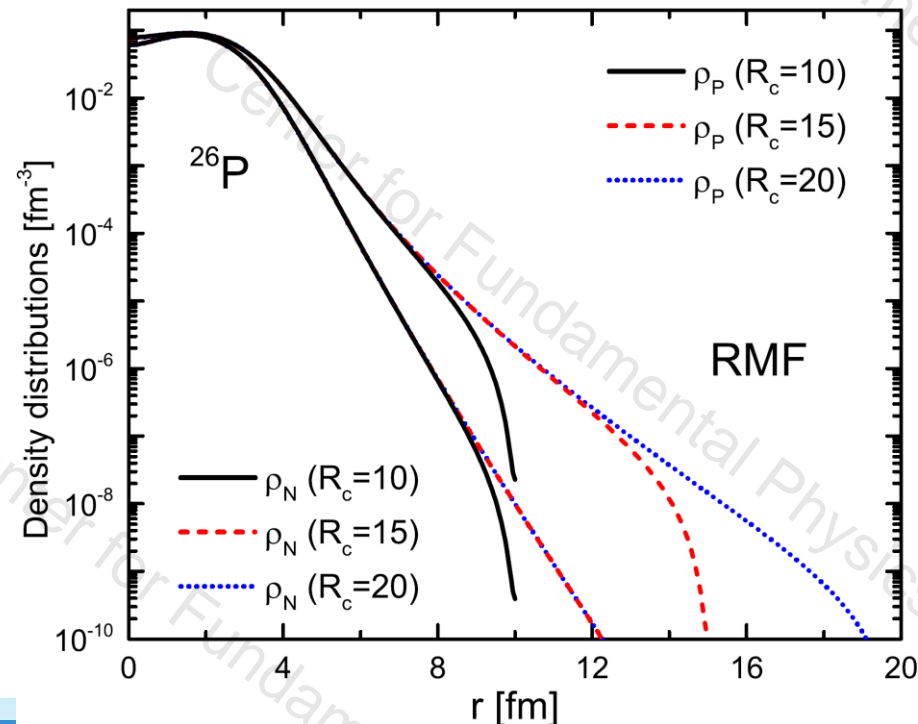
$$V_c^{\tilde{l}}(k, k') = \frac{\lambda}{\pi} \frac{Q_{\tilde{l}}(y)}{kk'}$$

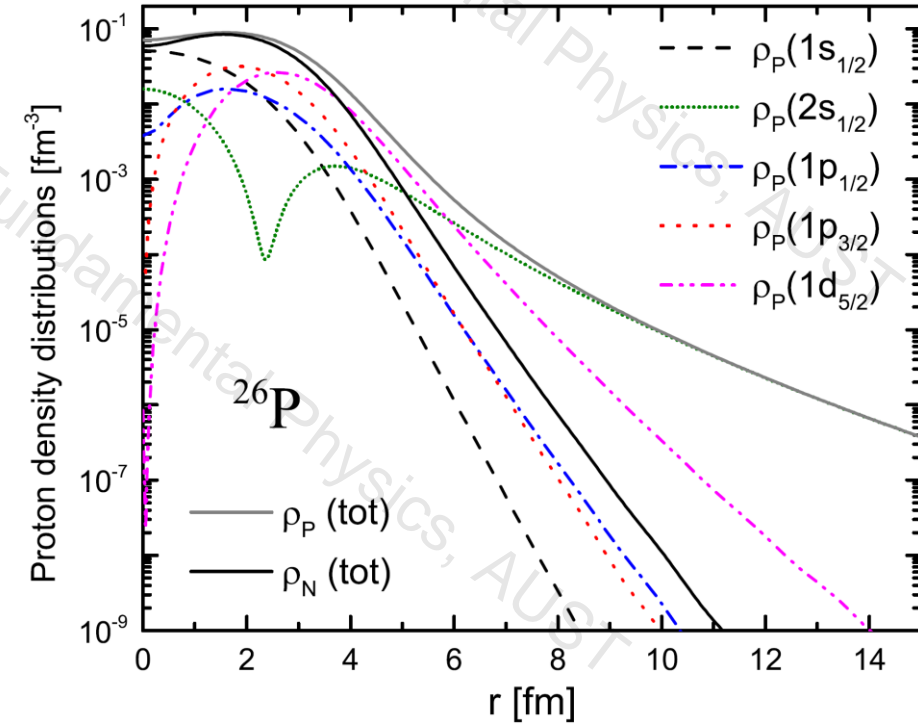
Comparison of RMF-CMR and RMF for density



- The density distributions in the RMF calculations depend on the box size.
- With the size of the box, the available density distributions are more dispersed, especially for protons.

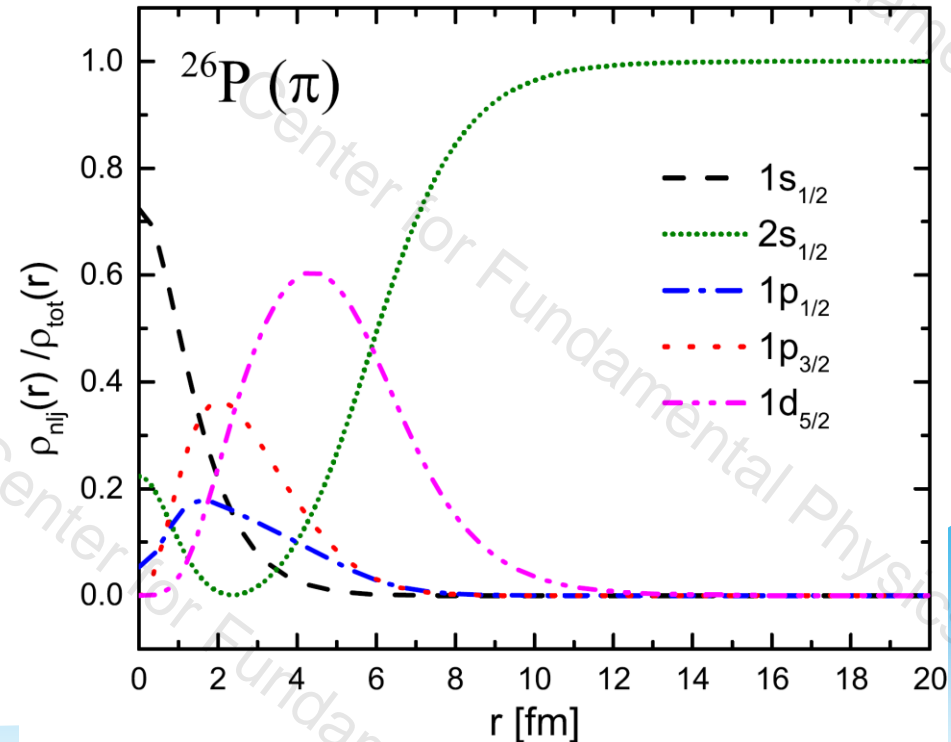
- The RMF-CMR calculation eliminates the dependence of the available density distributions on the box size.
- The proton density distribution in ^{26}P is more dispersed than that of neutron, i.e., there is a proton halo.



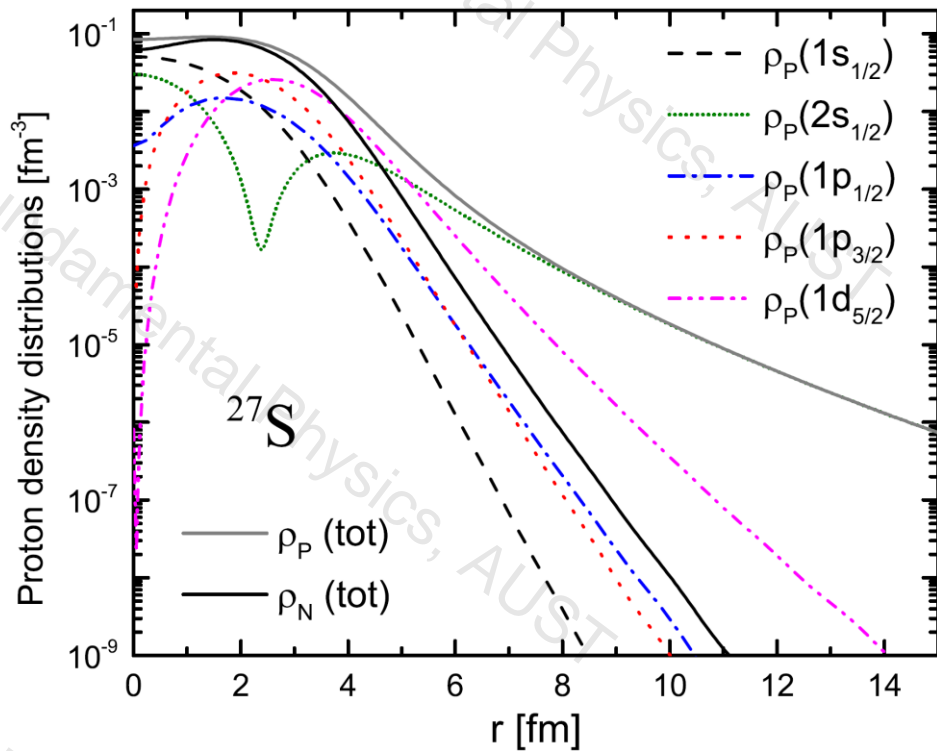


➤ The proton halo is mainly due to the occupation of the weakly bound level $2s_{1/2}$.

➤ The proton density distributions is more diffuse than that of neutron in ^{26}P , and there is a proton halo.

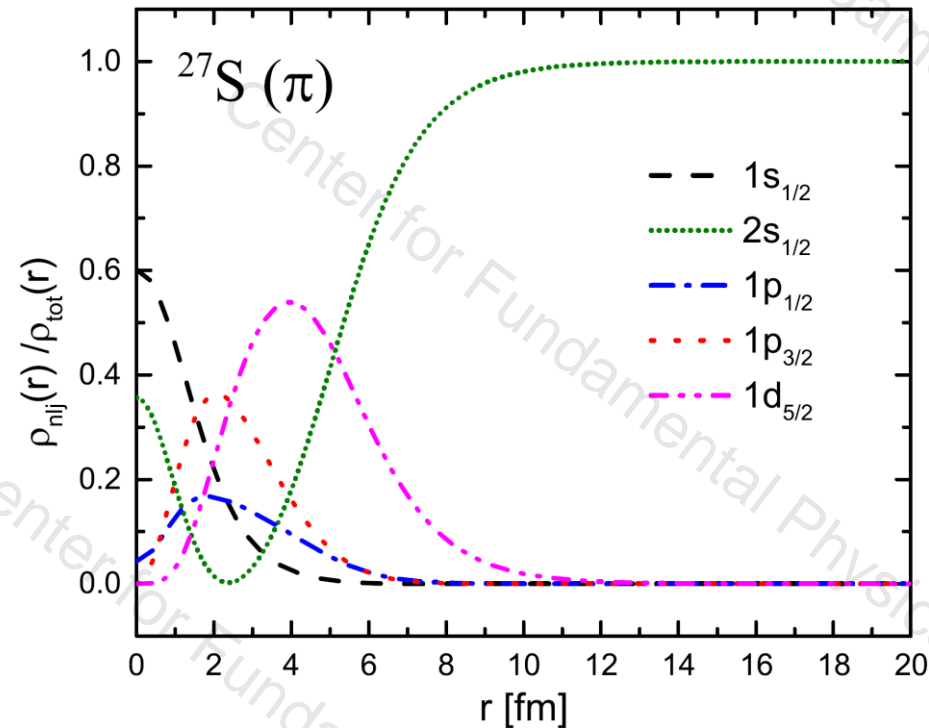


Exploration of proton halo in the S isotopes

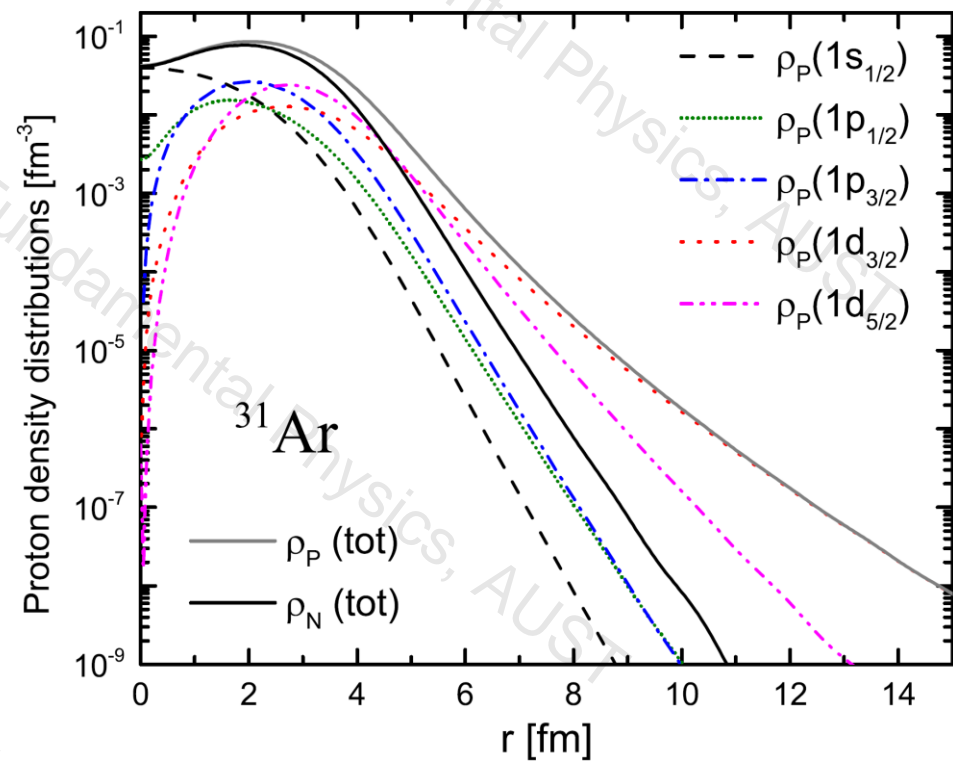


➤ The proton density distributions is more diffuse than that of neutron in ^{27}S , and there is a proton halo.

➤ The proton halo is mainly due to the occupation of the weakly bound level $2s_{1/2}$.

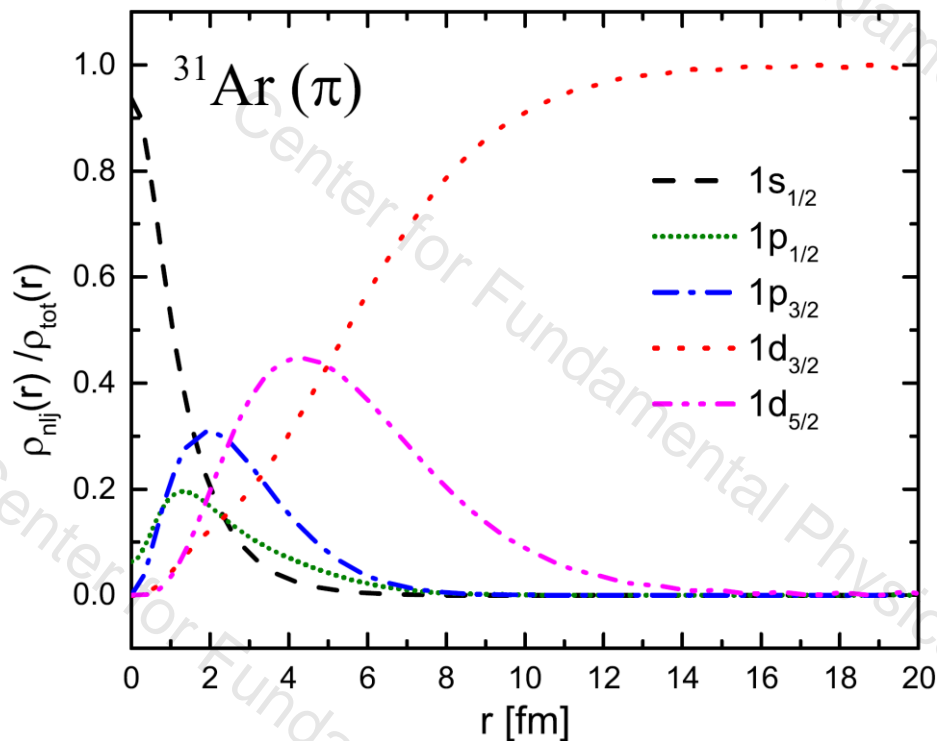


Exploration of proton halo in the Ar isotopes

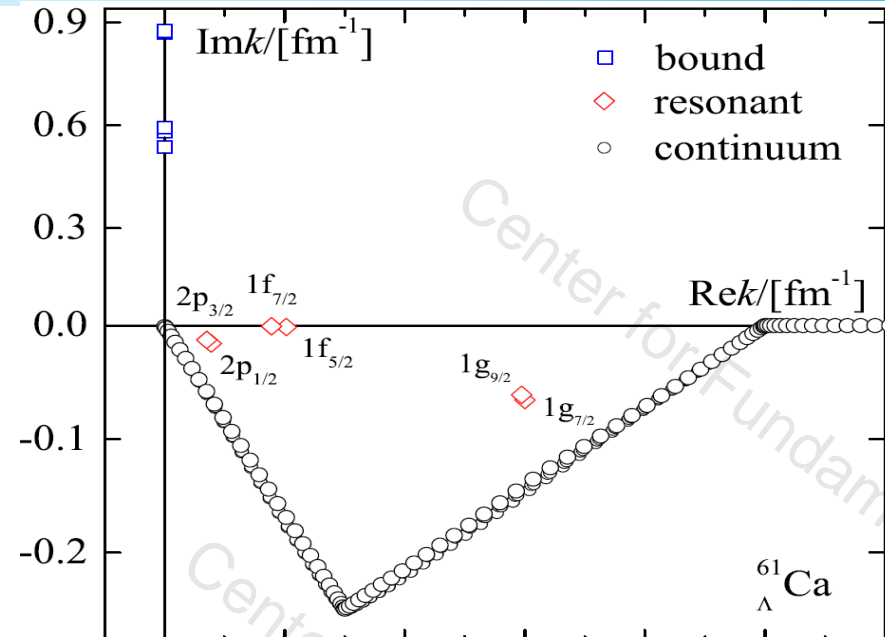
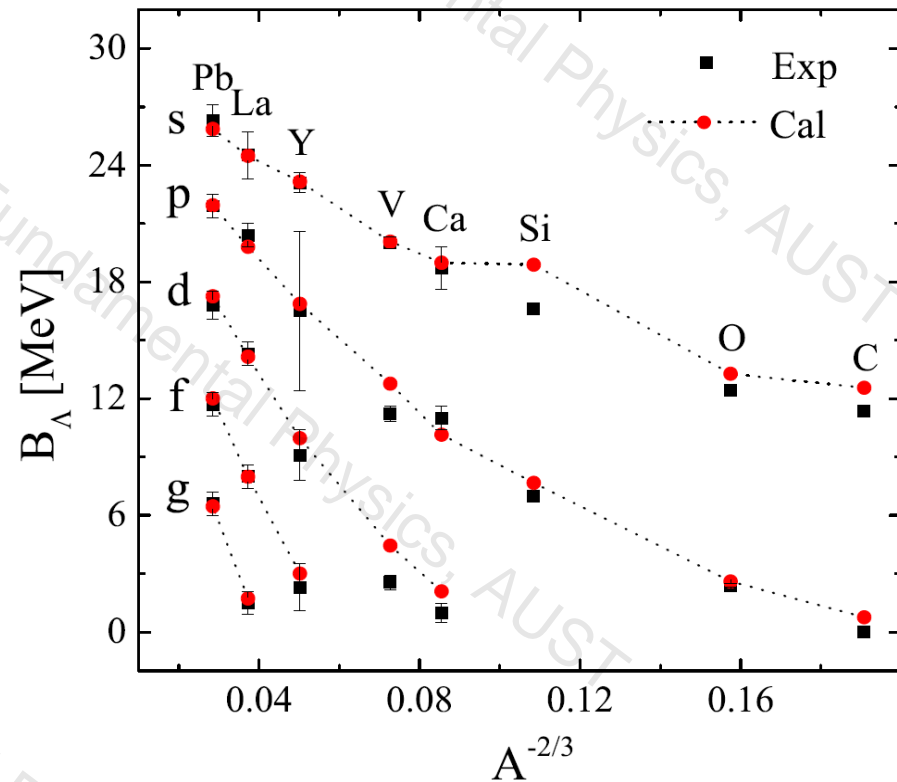


➤ The proton halo is mainly due to the occupation of the weakly bound level $1d_{3/2}$.

➤ The proton density distributions is relatively diffuse than that of neutron in ^{31}Ar . The proton halo phenomenon is not very remarkable.



Exploration of hyperon resonant states in hypernuclei



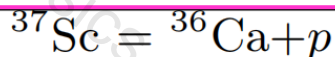
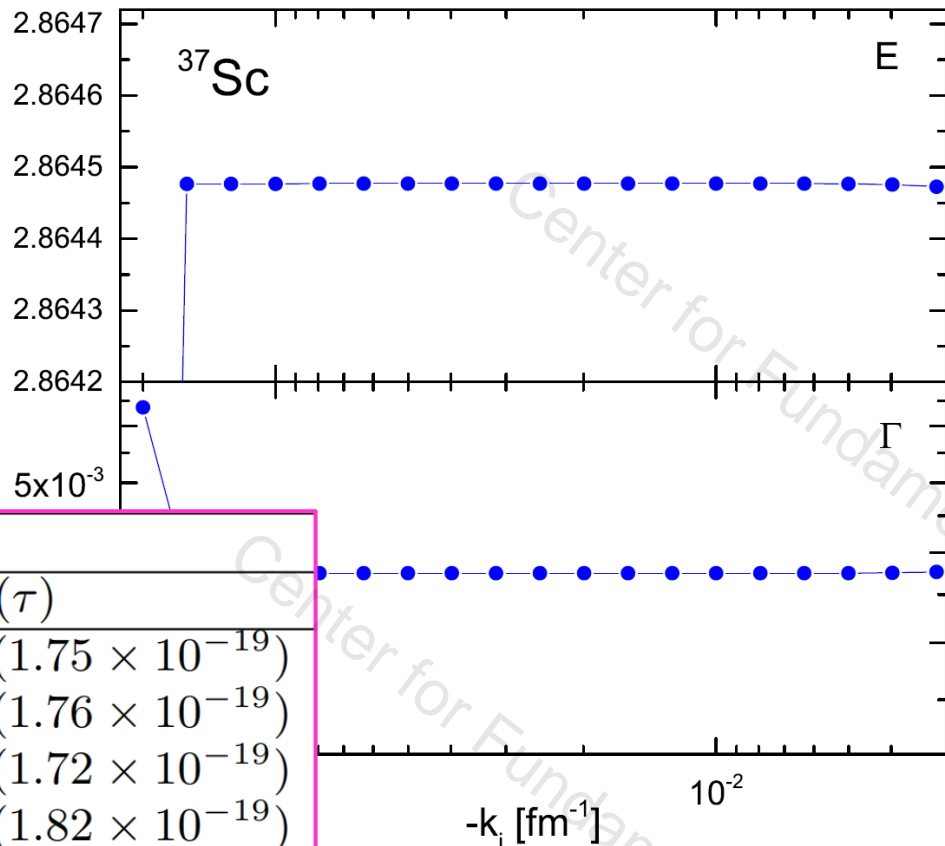
- The results for bound states are in agreement with the experiment.
- The results for resonant states are comparable to those from RMF-GF calculations [1].

[1] S.H. Ren, T.T. Sun, and W. Zhang, PRC 95, 054318 (2017)

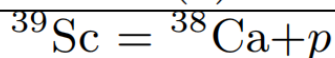
(a) ε_b	$1s_{1/2}$	$1p_{3/2}$	$1p_{1/2}$	$1d_{5/2}$	$1d_{3/2}$	$2s_{1/2}$
RMF-CMR	-20.7046	-13.4502	-13.2939	-6.1475	-5.9392	-5.0391
RMF-GF	-20.6035	-13.3109	-13.1363	-6.0358	-5.7893	-5.0977
(b) ε_r	$2p_{3/2}$	$2p_{1/2}$	$1f_{7/2}$	$1f_{5/2}$	$1g_{9/2}$	$1g_{7/2}$
RMF-CMR	0.0835	0.1006	0.5539	0.7148	6.0948	6.2005
RMF-GF	0.0774	0.1050	0.6147	0.8215	6.8017	6.9772
(c) Γ						
RMF-CMR	0.0617	0.0860	0.0076	0.0193	2.5220	2.7315
RMF-GF	0.1015	0.1259	0.0124	0.0229	3.2003	3.2926

Single proton emission

- The calculated energy and width as a function of the imaginary part of the vertex of the triangular contour $-k_i$.
- The upper (lower) panel represents the energy (width) of the $1f_{7/2}$ resonant state in ^{37}Sc .



Method	Q	$\Gamma(\tau)$
CMR	2.864	3.75×10^{-3} (1.75×10^{-19})
TD-Dirac	2.864	3.74×10^{-3} (1.76×10^{-19})
CSM	2.863	3.82×10^{-3} (1.72×10^{-19})
SM	2.863	3.62×10^{-3} (1.82×10^{-19})
experiment	2.9(3)	—

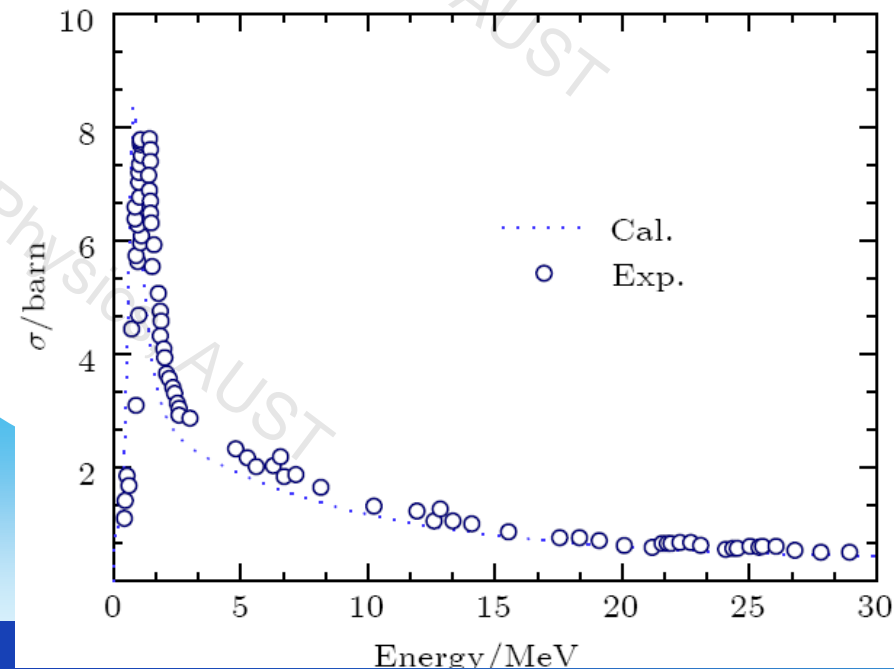
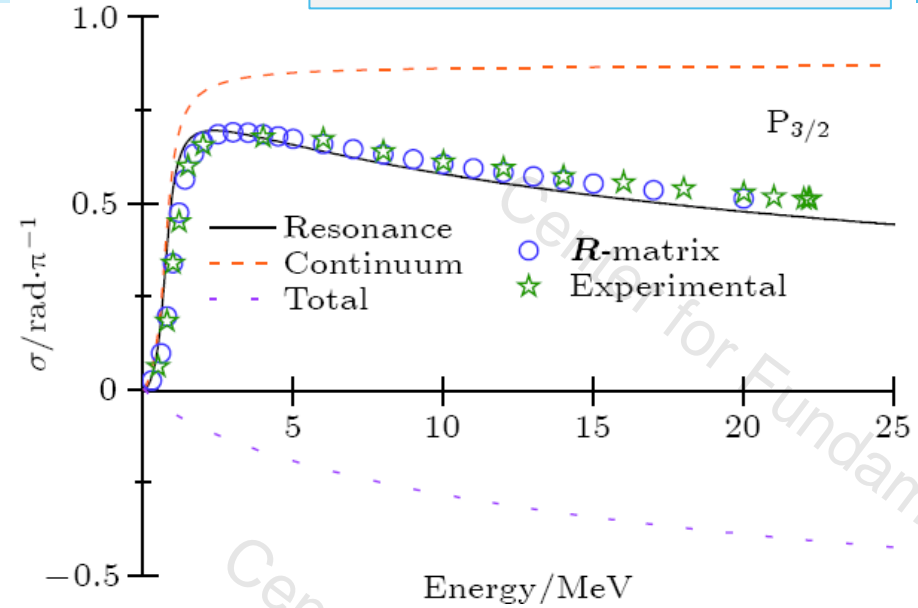
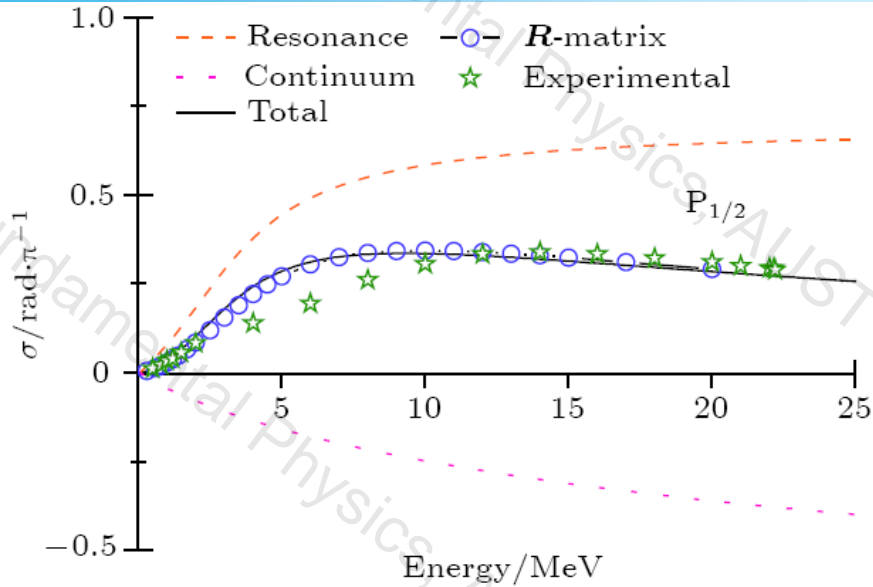


Method	Q	$\Gamma(\tau)$
CMR	0.664	3.88×10^{-9} (1.69×10^{-13})
TD-Dirac	0.662	3.87×10^{-9} (1.70×10^{-13})
experiment	0.597(24)	($\tau < 400$ ns)

- The Q value and decaying width of $1p$ emission evaluated in the $1f_{7/2}$ channel in comparison with the other methods.

◆ Calculation on scattering section

n- α scattering



- ◆ CMR is used to study the elastic scattering of **n- α** system, the continuum level density, phase shift, and cross section are obtained.
- ◆ The calculated results are in agreement with the experimental data.

- ◆ Significance of open quantum systems such as the nuclei far from the stability line is sketched. Some methods describing open quantum systems and their shortcomings are introduced.
- ◆ Formalism of RMF-CSM, RMF-CGF, and RMF-CMR are presented.
- ◆ Some applications on neutron, proton halos, and deformation halos discovered experimentally have been explained. Some possible exotic phenomena are predicted.

Thank you!



ELSEVIER

Contents lists available at ScienceDirect

Progress in Particle and Nuclear Physics

journal homepage: www.elsevier.com/locate/ppnp



Review

Recent development of complex scaling method for many-body resonances and continua in light nuclei

Takayuki Myo^{a,b,*}, Yumiko Yamamoto^c, Masahito Yamamoto^d, and Masahito Yamamoto^e

^a General Education, Faculty of Engineering

^b Research Center for Nuclear Physics (RCNP)

^c Nishina Center for Accelerator-based Science

^d Information Processing Center, Kitami Institute of Technology

^e Nuclear Reaction Data Centre, Faculty of Science



ELSEVIER

Contents lists available at ScienceDirect

Progress in Particle and Nuclear Physics

journal homepage: www.elsevier.com/locate/ppnp



Review

Bound state techniques to solve the multiparticle scattering problem

J. Carbonell^a, A. Deltuva^b, A.C. Fonseca^b, R. Lazauskas^{c,*}

^a Institut de Physique Nucléaire Orsay, CNRS/IN2P3, F-91406 Orsay Cedex, France

^b Centro de Física Nuclear da Universidade de Lisboa, P-1649-003 Lisboa, Portugal

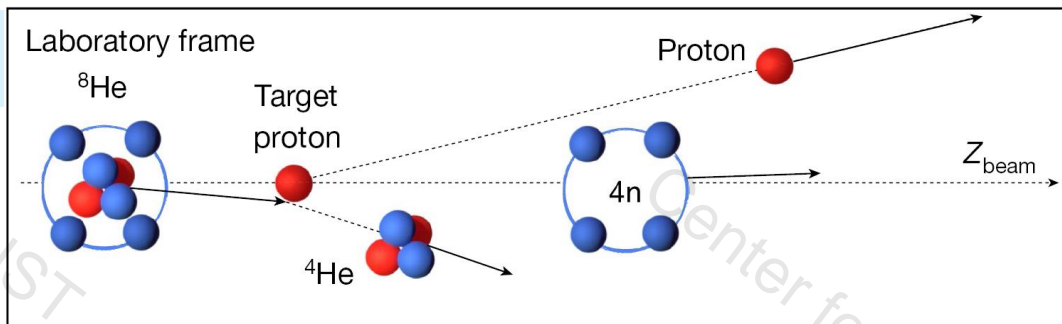
^c Université de Strasbourg, IPHC, CNRS, 23 rue du Loess, 67037 Strasbourg, France



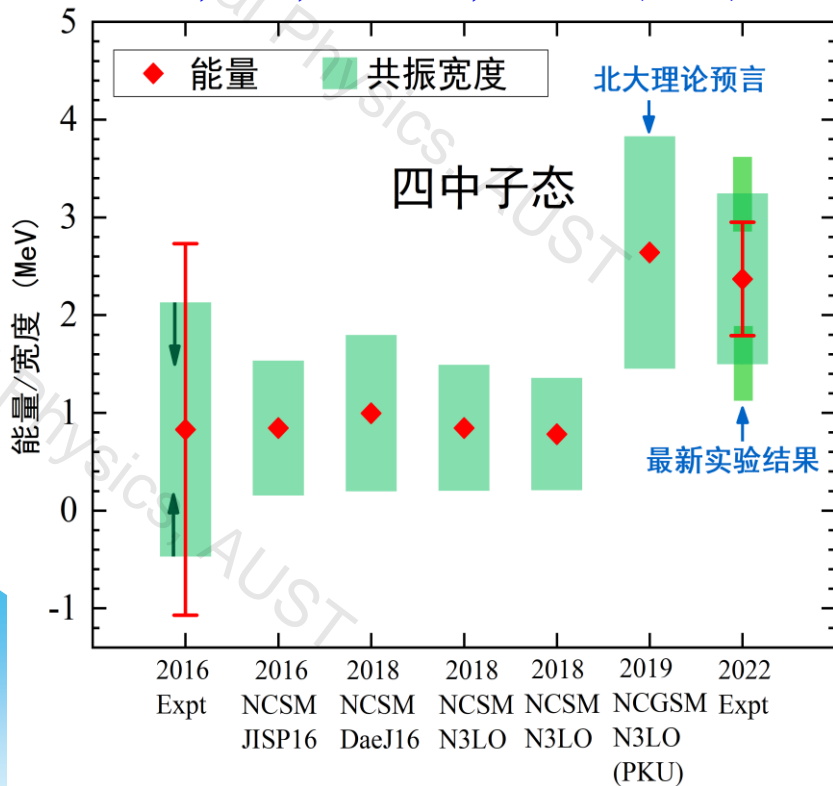
多中子 关联态

Tetraneutron

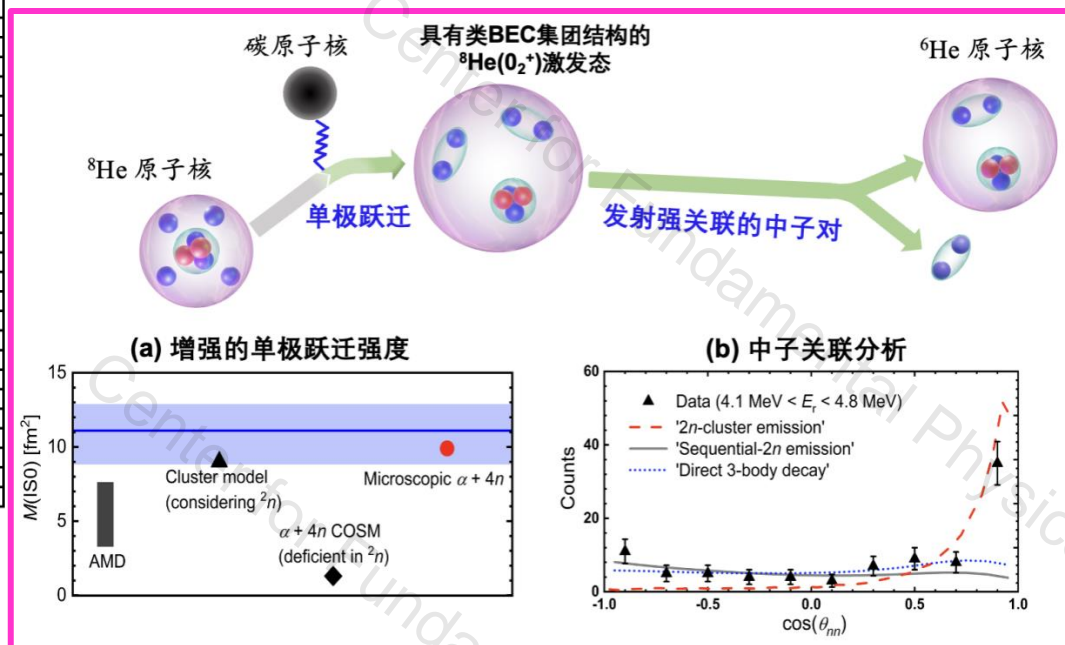
M. Duer et al.,
Nature (2022)



J.G.Li, et al., PRC100, 054313 (2019)

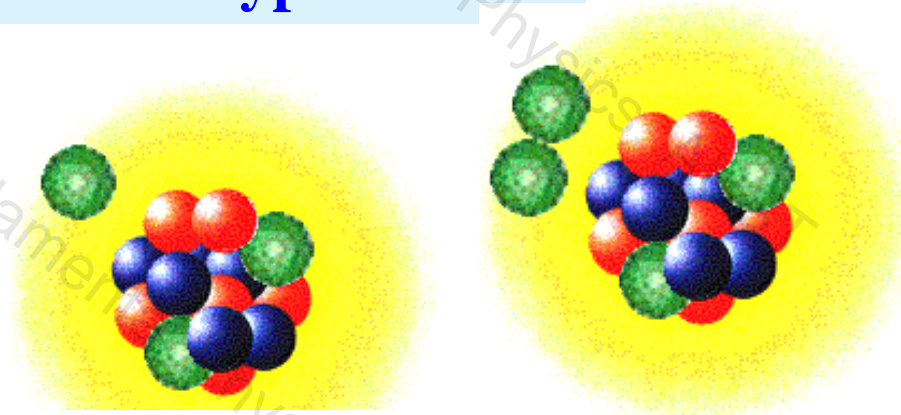


Z. H. Yang et al., PRL 131, 242501 (2023)



Halo in hypernuclei

Chart of Hypernuclides



<https://hypernuclei.kph.uni-mainz.de/>

